

Classification of Ice Hockey Skating Tasks using Kinematic Data

Matthew Kelly

Department of Kinesiology and Physical Education

McGill University

Montréal, Québec, Canada

A thesis submitted to McGill University in partial fulfillment of the requirements of the degree
of Master of Science

July 2021

© Matthew Kelly, 2021

Table of Contents

<i>Abstract</i>	4
<i>Abrégé</i>	5
<i>Acknowledgments</i>	6
<i>Contribution of Authors</i>	8
<i>List of Figures</i>	9
<i>List of Tables</i>	11
CHAPTER 1: INTRODUCTION & LITERATURE REVIEW	12
1.1 Introduction	12
1.2 Player Tracking Research	13
<i>1.2.1 Video-Based Player Tracking Research</i>	13
<i>1.2.2 Current Player Tracking Research</i>	16
1.3 Movement Patterns of Common Ice Hockey Skating Tasks	17
<i>1.3.1 Forward Skating Starts</i>	18
<i>1.3.2 Steady-state skating</i>	19
<i>1.3.3 Change of direction</i>	21
1.4 Skating Task Recognition	22
1.5 Objectives & Hypothesis	25
CHAPTER 2: METHODS	27
2.1 Participants	27
2.2 Data Collection	29
2.3 Machine Learning (ML) Models	30
2.4 Feature engineering	32
2.5 Model Segment Configuration	33
2.6 Model Performance Analysis	33
CHAPTER 3: RESULTS	37
3.1 Model and Segment Performance	37
3.3 Feature Importances	39
CHAPTER 4: DISCUSSION	41
4.1 Model Performance	41
4.2 Segment Performances	43
4.3 Feature Importances	44
4.4 Misclassifications	45
4.5 Limitations	45

CHAPTER 5: CONCLUSION.....	47
References	48
APPENDICES	52
Appendix A – Stop & Go Task Visual	52
Appendix B – Skating Start Task Visual	53
Appendix C – Skating Stride Task Visual	54
Appendix D – Wrist Shot Task Visual	55
Appendix E – Top Performing Models	56
Appendix F – Moderate Performing Models.....	58
Appendix G – Poor Performing Models	60
Appendix H – Feature Importances SVM Model Segments	62
Appendix I – Feature Importances RF Model Segments	65

Abstract

Professional ice hockey teams are adopting new technologies to gain a competitive edge. This includes tracking player game and practice movements by way of body worn sensor data. As yet, from these data there is no means of automating specific skating tasks identification. Hence, the purpose of this study was to evaluate whether data of players' body segment kinematics could be used to accurately identify skating tasks. Two machine learning models were used in classifying four ice-hockey skating tasks, to identify the body segment(s) data that could yield the highest classification performance. The models tested were a Support Vector Machine (SVM) and Random Forest (RF) model. The skating tasks classified were the 1) forward skating start, 2) forward skating strides, 3) skating stop & go and 4) skating into a wrist shot. From previous studies, full 3D body kinematic skating data of ice hockey players were pooled. These data included skaters' lower body and trunk segment center of mass' linear accelerations. Results showed that the RF model performed better with F1 scores ranging from 96.3 to 97.6% compared to the SVM model with f1 scores ranging from 69.1 to 96.8% in classifying the on-ice tasks while lower extremity segments (foot, shank and thigh) had the highest classification scores. These results demonstrate the potential of using body segment kinematic measures to auto-identify specific skating tasks in combination with monitoring an athlete's workload.

Abrégé

Plusieurs équipes professionnels de hockey sur glace collecte des données de mouvement durant les parties et pratiques avec de captures spatiale sur le corps, mais n'ont pas encore de méthode automatique pour définir les tâches spécifique de patinage durant c'est mouvements. Par conséquent, l'objectif de ce projet était d'évaluer si des données de segment de corps des joueurs (centre de masse des cuisse et jambe) pourrait être utiliser pour identifier des tâches de patinage. Deux modèles d'apprentissage automatique ont été utiliser pour classifier quatre tâches de patinage de hockey sur glace et pour identifier les segments de corps qui ont donnés les plus hautes performance de classification. Les modèles testé était le Support Vector Machine (SVM) et Random Forest (RF). Les tâches de patinage classifié était 1) accélération avant, 2) vitesse maximale avant, 3) "stop & go" et 4) tirs du poignet en patinant. Les données kinématiques 3D de tout le corps de patinage des joueurs de hockey sur glace a été groupé de projects de capture de mouvement sur glace précédent. Ceci a inclut l'accélération linéaire du centre de masse des segments du corps des joueurs. Les résultats ont montrés que le modèle RF a mieu performé avec des notes de f1 entre 96.3 à 97.6% comparé au modèle SVM avec des notes f1 entre 69.1 à 96.8% au terme de classifier les tâches sur glaces; pendant que les segments en extrémité (pied, jambe et cuisse) avait les notes de classification les plus hautes. Ces résultants démontre le potentiel de l'utilisation des mesures kinématiques de segment du corp pour l'identification automatique des tâches de patinage en combinaison avec les métriques de suivies de tout le corps. Cette information peut améliorer la prise de décision pour les entraîneurs et formateurs en terme de compétence et formation physique.

Acknowledgments

First and foremost, I want to acknowledge and thank all front-line healthcare workers for your unselfish contribution to helping so many people affected by the COVID-19 pandemic. Words will never be able to express how thankful I am for you. I also want to thank all medical researchers who have contributed to developing a timely and effective vaccine, as well as all workers and volunteers who have contributed to the global distribution and vaccination of people all over the world. Thanks to you, a return to normalcy is in sight.

Next, I would like thank Dr. David Pearsall for giving me the opportunity to be a part of the IHRG and for helping me develop as a researcher within a sport that I am deeply passionate about. A huge thank you to Philippe Renaud for all your help, support and patience over the past 2 years. Through some trial and lots of errors, we got it done. Another big thanks to Philippe Dixon for your guidance and expertise in machine learning and python, having you onboard was an absolute game changer for the quality of my project.

To my lab mates; Dan Aponte, Cait Mazurek, Aimée Quintana, Aaron Manning and Sean Denroche, thanks for showing me the ropes of the IHRG and for all the great in-lab and out-of-lab pre-pandemic memories. The BBQ boys a.k.a Taylor Léger and Harry Brown, thank you for the lengthy educational discussions and for helping me navigate through progress reports, class registrations and all the other things I likely never would've completed. Literally wouldn't be writing this today if it weren't for you guys.

A special thank you to all my friends and family back home, especially Elliot and Scarlett, whom I've yet to meet. Being away from such important people in my life is not easy, but all your love and support has kept me pushing forward.

Last but not least, Mom and Dad. Thank you for your endless love and support. I will forever be grateful for all you have done for me and provided for me. Thank you for gifting me with endless opportunities to explore and grow as a person, for believing in me and trusting I will make the right life decisions even though you don't always know exactly what I'm doing or where I'm heading next. I love you both.

Contribution of Authors

Matthew Kelly, MSc. Candidate, Department of Kinesiology and Physical Education, McGill University, was responsible for the research design, processing and analysis of data and the writing of this thesis. The candidate's supervisor, David J. Pearsall, PhD, Associate Professor, Department of Kinesiology and Physical Education, McGill University, contributed to the research design and analysis of the data.

Philippe C. Dixon, PhD, Assistant Professor, School of Kinesiology and Physical Activity Sciences, Université de Montréal, contributed to the research design and helped to develop the machine learning models. Dr. Shawn Robbins, PhD, Assistant Professor, School of Physical and Occupational Therapy, McGill University and Dr. Richard Preuss, Assistant Professor, School of Physical and Occupational Therapy, McGill University were members of the thesis advisory. Philippe J. Renaud, MSc., Department of Kinesiology and Physical Education, McGill University, played a very important role in the research design, data collection and data analysis, acting as the lab research assistant.

List of Figures

Figure 1 Summary flow chart of smart sensor adapted from Mendes et al. (2016).....	22
Figure 2 Example of a linear SVM ML model (Garreta & Moncecchi, 2013).....	31
Figure 3 Simplified example of a decision tree ML model (Genuer et al., 2008).	32
Figure 4 A simplified flow chart demonstrating the step-by-step process of evaluating a ML model performance (adapted from Mannini and Sabatini (2010)).	36
Figure 5 Example confusion matrices of the top performing foot segment from the 10-fold cross validation SVM and RF models (See Appendix E-G for top, moderate and poor performing models from all segment models).	38
Figure 6 Top 10 feature importances (mean and standard deviation) of the SVM and RF models for the top performing foot segment (See Appendix H and I for feature importances of other segment models).	40
Figure 7 Visual representation of stop & go task from Hallihan (2018).	52
Figure 8 Visual representation of skating start task from Shell et al. (2017) and Renaud et al. (2017).....	53
Figure 9 Visual representation of skating stride task from Budarick et al. (2018).....	54
Figure 10 Overhead and sagittal visual representation of wrist shot task from Robbins et al. (2020).....	55
Figure 11 Example confusion matrices of top performing models from the 10-fold cross validation of a) all segments b) trunk segment c) thigh segment d) pelvis segment e) foot segment f) shank segment.	57
Figure 12 Example confusion matrices of moderate performing models from the 10-fold cross validation of a) all segments b) trunk segment c) thigh segment d) pelvis segment e) foot segment f) shank segment.	59
Figure 13 Example confusion matrices of poor performing models from the 10-fold cross validation of a) all segment b) trunk segment c) thigh segment d) pelvis segment e) foot segment f) shank segment.	61
Figure 14 Top 10 feature importances (mean and standard deviation) of the SVM model for a) all segment b) trunk segment c) thigh segment d) pelvis segment e) foot segment f) shank segment.	64

Figure 15 Top 10 feature importances (mean and standard deviation) of the RF model for a) all segment b) trunk segment c) thigh segment d) pelvis segment e) foot segment f) shank segment
..... 67

List of Tables

Table 1 Participant and task characteristics (See Appendix A-D for task visual representations).	28
Table 2 Motion capture camera and marker set up.	29
Table 3 Data processing criteria.	30
Table 4 Features engineered and input into ML model.	33
Table 5 Mean percentage (standard deviation) of model performance for the six segment configurations. The “All” sensor configuration combines input from the five individual segments. Highest average scores are in bold.	37
Table 6 Mean percentage (standard deviation) of model performance for the six segment configurations. The “All” segment configuration combines input from the five individual segments. Highest average scores are in bold.	38

CHAPTER 1: INTRODUCTION & LITERATURE REVIEW

1.1 Introduction

Ice hockey is known as Canada's national sport, with over 600,000 young Canadians registered in the sport every year (IIHF, 2021). But hockey is in fact a well-known sport around the world, with over 1.7 million players registered world-wide every year (IIHF, 2021). The sport of hockey has evolved with advances in technology, mostly in equipment materials and design, but also with smart technologies. As well, sports analytics have become an important driver of decision-making by major stakeholders in sports, the evolution of coaches' ability to use data. Technology in hockey is changing the game.

Business endeavours such as SportLogiq, Catapult and Kinduct have been at the forefront of revolutionizing real-time tracking of individual and group sport practice and game dynamics movements. For example, the system developed by SPORTLOGiQ (SPORTLOGiQ, 2021) is changing our approach to coaching team tactics and player development by providing fast and actionable in-game metrics such as passes to the slot, dump-in recoveries and entry success/denials. Catapult (Catapult, 2021) has developed a wearable technology that provides data on player speeds, distances covered and external workload which can all be used in improving athlete health, recovery and physical performance. Kinduct (Kinduct, 2021) created a digital dashboard that integrates data from many different systems and technologies into one condensed user-friendly platform for rapid access and interpretation of data.

Long gone are the days of tedious and subjective tracking of players' performance by way of pen and paper. Now with automated wireless and/or video player movement data acquisition systems, we are making leaps and bounds in the precision and amount of tracking data available that can provide tangible assessment of individual and team players' movements.

Current methods of player tracking utilize video-based task recognition, accelerometers and/or local positioning systems (LPS) to provide data on player's movements on the ice but are not necessarily able to provide physical performance data (e.g. speed, distance, workload, etc.) specific to hockey-related tasks performed (e.g. start, stop & go, crossover, etc.). To address this deficiency, machine learning (ML) has shown the potential to identify specific tasks executed.

Hence, the purpose of the current study was to compare different ML models using different combinations of lower body 3D movement data to determine the accuracy of each ML model in the classification of different hockey tasks and their accuracy based on model F-1 scores. Initially, a review of the literature was carried out to establish the current state of research on player tracking focusing on the use of machine learning on sports, particular in sports with stride-like movements.

1.2 Player Tracking Research

1.2.1 Video-Based Player Tracking Research

Early in-game player tracking research of ice hockey used post-hoc time-motion observational analysis of game videos to describe player and game characteristics. For example, from game video recordings Bracko, Fellingham, Hall, Fisher, and Cryer (1998) visually identified skating tasks' prevalence and duration used by professional hockey players. They observed skating task profile characteristic of six high-point scorers and six low-point scorers. The authors reviewed video of the second period from two NHL regular season games. Each player shift was reviewed in slow-motion first to record skating characteristics and again to record the amount of time spent in each characteristic. Similarly, post-hoc video analysis was used by Montgomery, Nobes, Pearsall, and Turcotte (2004) for hockey task analysis of 10 NHL teams during 9 NHL games. They quantified the time and frequency of various skating, shooting,

passing and hitting tasks across player positions. Similarly, Wennberg (2004) used 22 game videos from the NHL finals, World Junior Championships and Winter Olympics between 2001 and 2002 to compare collision frequency in elite hockey games on North American and International rink size. However, as relevant as this information may be, post-hoc video analysis of in-game player activity is extremely time consuming; for example requiring 120 minutes of observation to review all activities during one minute of game play (Montgomery et al., 2004). This method is also prone to research observer's bias in skating event identification; hence, results can be difficult to replicate. Since then, great effort has been given to developing hardware and software technologies towards the goal of real-time task and movement player analysis. To achieve this, more recent player tracking studies have explored the use of artificial intelligence algorithms to assess video-based and/or smart sensor player worn data for task game analysis identification.

In an attempt to develop a video-based system to identify multiple hockey players in-frame and classify their actions, Lu, Okuma, and Little (2009) used Hue-Saturation-Value (HSV) and Histogram Oriented Gradients (HOG) models to capture the color of the player and encode the shape of the player, respectively. Subsequently, they adopted a Switching Probabilistic Principal Component Analysis (SPPCA) template to continuously update and adjust the template as the targeted player moves on video. Action recognition was performed by computing a frame-by-frame similarity matrix between testing and training HOG descriptors which was input into a Sparse Multinomial Logistic Regression (SMLR) classifier. Comparing player shape to identify the player's action, the classifier would then classify the template as skating up, down, left or right on the video. Testing a variety of parameter settings, the accuracy of the system ranged from 52.42% to 76.37%.

Building off the work of Lu et al. (2009), Fani and Neher (2017) believed that using player pose might be a better approach in recognizing higher level hockey features like shooting and crossovers. Their approach consisted of a 3-layer deep convolutional neural network (CNN) known as an Action Recognition Hourglass Network (ARHN). This network can be reduced to three components: 1) the stacked hourglass network where raw images are input into the network and the player pose is defined by using statistical heatmaps to estimate joint positions, 2) the latent transformer receives the estimated pose and transforms them to a common frame of reference, and 3) the action classifier which identifies the player action (Fani & Neher, 2017). The accuracy of the model on classifying straight skating, crossovers, pre-shot and post-shot ranged from 65.14% to 78.49%. The authors found that the model commonly misclassified similar tasks, thus by merging these tasks (skating with crossover and pre-shot with post-shot) the model accuracy improved. This suggests that using player pose may work well with contrasting tasks, such as shooting and skating, but less well with tasks that have similar actions.

Notwithstanding these substantial advances noted, video-based human activity recognition does have drawbacks. First, multiple studies have commented on certain techniques leading to a lost accuracy of the player location on the field of play (Lu et al., 2009; Schulte et al., 2017). Specifically, identifying a player outline in a white uniform may prove difficult against the white background of the boards and ice of an arena. Additionally, Vrigkas, Nikou, and Kakadiaris (2015) express other challenges with using video like background clutter, player occlusion, changes in scale, frame resolution and lighting. An alternative to these outstanding video base problems are the adoption of wearable and wireless tracking technologies.

1.2.2 Current Player Tracking Research

Many current player tracking systems used in sports today involve global and/or local positioning measurement technologies. For example, Global Positioning Systems (GPS) were first applied in a team sports setting in 2003 (Larson, 2003) and have led to the ability to track player position, distance covered, speed, workload, etc. in real-time. While GPS have been validated for outdoor player tracking (Scott, Scott, & Kelly, 2015), indoor sports' building structures create signal interference from orbiting satellites, degrading accuracy in player tracking (Larson, 2003). Thus, Local Positioning Systems (LPS) are more commonly used for indoor sports. These devices use technologies such as Radio Frequency Identification (RFID), Wireless Local Area Network (WLAN), Bluetooth and Ultra-wideband (UWB) (Serpiello et al., 2018). UWB has been validated for use on indoor courts (Luteberget, Spencer, & Gilgien, 2018; Serpiello et al., 2018) and has been successfully used on the ice with hockey players (Douglas & Kennedy, 2019)

Douglas and Kennedy (2019) tracked in-game movement in 20 U20 elite hockey players using the UWB technology to measure skating distances covered and skating speed over 5 games. Other studies measuring in-game hockey movement have used accelerometers. For instance, Douglas, Rotondi, Baker, Jamnik, and Macpherson (2019) measured PlayerLoad, PlayerLoad/minute, explosive efforts and training impulse in 25 elite female hockey players in over 100 ice sessions using accelerometer data. These metrics provide trainers and coaches with valuable in-game measures of player effort during periods of high or low intensity and fast or slow speeds. Better yet would be to identify concurrent acceleration measures with specific hockey tasks.

In addition, more robust accelerometer sensors in hockey have the ability to track player events such as player impacts. For example, Pilotti-Riley, Stojanov, Sohaib Arif, and McGregor

(2019) used accelerometers to track and measure in-game player incurred impacts in 23 U18 national hockey team players. Similar accelerometers have previously been used in identifying skating stride elements like contact time, stride time and measure stride propulsion (Stetter, Buckeridge, Nigg, Sell, & Stein, 2019; Stetter, Buckeridge, von Tscharnner, Nigg, & Nigg, 2016). Therefore, having accelerometers worn by players may be able to identify skating tasks such as starting, forward skating and stopping. Thus, body worn sensors have the potential to provide a deeper understanding of the biomechanics of such skating tasks in-game player tracking data. Further study is needed to determine how accurately skating tasks can be classified as well as to identify what specific data are needed to classify accurately.

1.3 Movement Patterns of Common Ice Hockey Skating Tasks

In order to classify different skating tasks, body movement pattern data (e.g. kinematic joint angle-time patterns) can be used. Movements of body segments about joints are produced by periodic accelerations (generated internally by muscles and externally imposed by the environment). Few studies have specifically compared joint kinematic differences of skating tasks or differences in their adjacent segment accelerations. However, previous studies have individually examined tasks such as skating starts, full strides and change of direction tasks. These common skating movement patterns will be further explored in the upcoming sections as these were the tasks input into the ML model of the current study and attempted to classify using kinematic data.

The forward skating stride can be broken down into phases: glide, push and recovery. The glide (stance) phase consists of the skater support limb maintaining a flexed hip and knee position, followed by the push off phase consisting of an explosive extension of support limb's hip and knee, and lastly the recovery (swing) phase bringing the leg forward (hip and knee

flexion) under the body and on to the ice in preparation to for push off on the contralateral leg (Boer & Nilsen, 1989).

1.3.1 Forward Skating Starts

Forward skating is the most fundamental method of locomotion in ice hockey. Equally important is the ability to rapidly accelerate (e.g. “starts”) prior to achieving steady state (constant velocity) skating (Budarick et al., 2018; Koning, Thomas, Berger, Groot, & Ingen Schenau, 1995). Three basic hockey starts exist: straight forward “V”, crossover and “T” starts, with the most commonly used being the forward and crossover start (Pearsall, Turcotte, & Murphy, 2000). Where the crossover start consists of 1 to 2 steps crossing one foot over the other. Koning et al. (1995) describes the forward skating start as similar to a running sprint; that is, the extension of the legs occurs in the opposite direction than the intended skating direction to create forward progress. Skater’s start movements typically show rapid short steps and periodic flight phases (McPherson, Wrigley, & Montelpare, 2004; Renaud et al., 2017). To overcome the ice’s low coefficient of friction skaters will externally rotate and abduct their hip, knee and ankle to “dig” their blade edge into the ice to accelerate their body center of mass both forward and upward (Buckeridge, LeVangie, Stetter, Nigg, & Nigg, 2015; Renaud et al., 2017). The start phase occurs over the first 3 to 6 steps before transitioning to steady state skating (Koning et al., 1995; Marino, 1983; Pearsall et al., 2001; Renaud et al., 2017). During this transition, knee flexion gradually increases with each stride, ranging from 21° at first push-off to 63° at third push-off, to lower skater’s center of mass (Lafontaine, 2007). This start technique is also shown by speed skaters to achieve greater hip and knee extension velocities (Koning et al., 1995). The ankle remains dorsi-flexed (12°-16°) and everted during the initial steps. (Lafontaine, 2007).

The earlier work in ice hockey skating biomechanics by Marino (1983) identified mechanical factors that were good predictors of fast acceleration times: these included high stride rates, forward body lean at ice contact, and decreased single support phase and recovery foot placement under the body. McPherson et al. (2004) found that, increased knee flexion at touchdown, decreased skate push-off angle, increased knee extension and hip abduction at push-off and greater forward lean are positive predictors of acceleration in youth hockey players.

Recent 3D motion capture studies have examined ice hockey starts. In the sagittal plane, high caliber skaters demonstrate greater hip extension at push-off, which would also coincide with greater forward trunk lean, and greater knee extension velocity (Buckeridge et al., 2015; Marino, 1983; McPherson et al., 2004). High caliber players show higher stride rate and short double support times (Buckeridge et al., 2015; Renaud et al., 2017). In the frontal plane, greater hip abduction velocities contributed to higher skater's center of mass velocity (Renaud et al., 2017).

1.3.2 Steady-state skating

After the acceleration phase, skating mechanics transition from a “running” start to more of a push and glide motion (Buckeridge et al., 2015; Budarick et al., 2018; Koning et al., 1995). This transition has been characterized by increased glide time during push-off and a more lateral push-off with more plantarflexion in speed skaters (Koning et al., 1995). In ice hockey, the transition from start to steady state demonstrated increasingly greater side-to-side movement of the center of mass, also suggesting a more lateral push off (Budarick et al., 2018). This is supported from kinematic measures showing greater hip abduction range of motion (ROM) and velocity, in addition to greater knee ROM (Buckeridge et al., 2015). The transition also shows a change from unimodal stance phase acceleration patterns during the acceleration phase to

bimodal stance phase acceleration patterns during steady state skating (Buckeridge et al., 2015). Negative glide acceleration is a result of friction between the ice and skate blade and drag resistance (Budarick et al., 2018; McPherson et al., 2004). Similarly, a transition from unimodal to bimodal ground reaction force (GRF) kinetic curves is observed, from unimodal GRF patterns during acceleration and bimodal GRF patterns in steady state skating (Stidwill, Turcotte, Dixon, & Pearsall, 2010). These force patterns demonstrate a transition from a “running” step in acceleration to a push and glide step in steady state skating.

1.3.3 Change of direction

Stops and starts are a common tactic to change quickly directions in ice hockey. As starts have already been addressed above, this section's focus will be on stops. In order to quickly decelerate, skaters rotate and laterally dorsiflex both ankles to position the skate blades perpendicular to the direction travelled and “dig” the blade's edges into the ice (Fortier, Turcotte, & Pearsall, 2014; Pearsall et al., 2000). Almost simultaneously, skaters will laterally tilt the pelvis towards the inside (trailing) leg while laterally tilting and rotating the trunk in the opposite direction to maintain stability all while lowering their CoM by flexing the trunk and the inside leg hip and knee (Hallihan, 2017). Increased iced friction is achieved by applying a greater vertical GRF by way of the outside skate pressing laterally (thereby creating a medial reaction force) and conversely the inside skate presses medially (thereby creating a lateral reaction force) (Fortier et al., 2014). Reaction forces on the outside leg are twice as high than the inside leg (Fortier et al., 2014) suggesting that the inside leg may play more of a role in maintaining balance during the maneuver (Forget, 2013). Using pressure insole sensors, high caliber players show greater pressure on the heel and less center of pressure excursion compared to low caliber players, suggesting better postural control during the stop (Forget, 2013). They also apply greater vertical force on the outside skate allowing them to stop faster (Forget, 2013), which may give them an advantage in transitions over a lower caliber opponent.

In summary, the above studies confirm that kinematic measures of lower body segments and joints are distinct between different skating tasks (e.g. forward skating starts, steady state skating, starts and stop, stop and go transitions). This intuitively makes sense; thus, inversely it is conceptually feasible that kinematic “signature” measures of lower body segments and joints and body center of mass movements can be used to predict the type and quality of skating tasks.

1.4 Skating Task Recognition

The implementation of wearable technology in sports has allowed for key stakeholders to freely collect data on players to improve performance and reduce the risk of injury (Hulin, Gabbett, Lawson, Caputi, & Sampson, 2016). Wearable sensor systems such as inertial measurement units (IMUs), characterized by their ability to wirelessly transmit useable data to the end user (Mendes, Vieira, Pires, & Stevan, 2016), allow for data collection within larger areas (e.g. full playing field) compared to traditional passive marker systems. Data acquired via wearable sensors can be filtered and processed before being communicated to the user via cable or wirelessly (e.g. Bluetooth®), making data ready to use once it reaches the end user (Figure 1) (Mendes et al., 2016). Furthering the use of rapidly accessible data, classification of tasks using machine learning algorithms can provide some context to the data analyzed by the user.

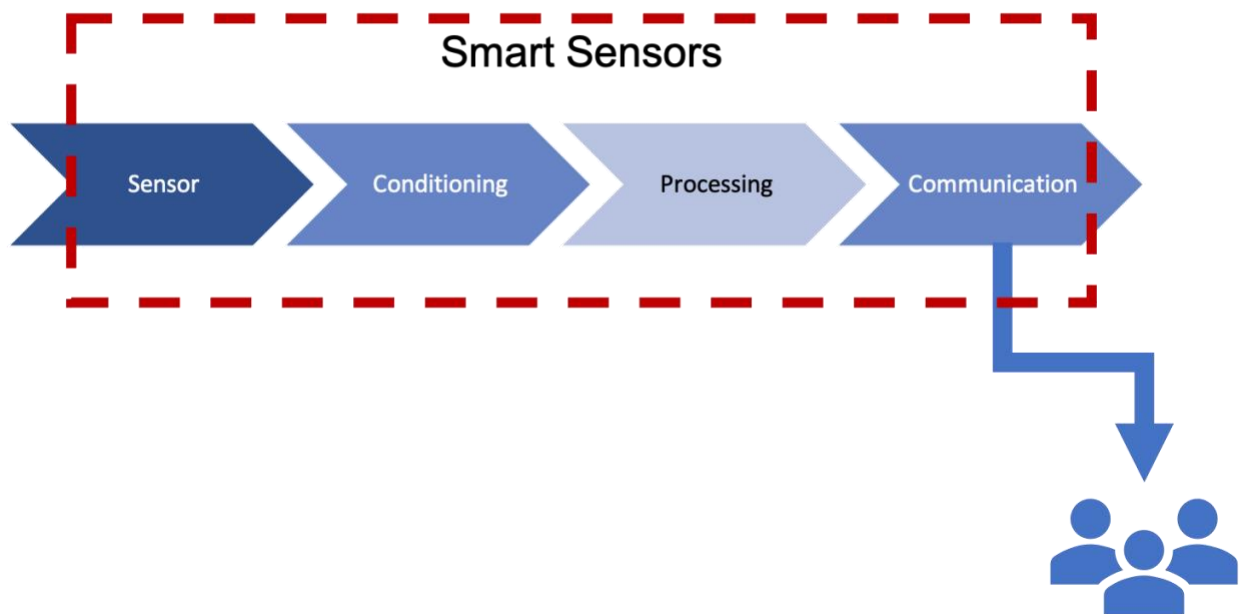


Figure 1 Summary flow chart of smart sensor adapted from Mendes et al. (2016).

Previous literature using accelerometers has demonstrated the possibility of using wearable sensors for the classification of skating tasks. Hardegger et al. (2015) conducted a study of skating task recognition in inline and ice hockey players. IMUs were placed on the participants skate laces to identify jumps, turns, breaking, sharp turns, crossovers, backward skating and power strokes from acceleration and velocity data. They found that a random forest classifier performed best for classifying the skating tasks, with an overall F1 score of 0.9 for inline skating and 0.7 for ice skating tasks, where F1 score is the harmonic mean of precision and recall (Hardegger et al., 2015).

The large difference between the inline and on ice tasks could be explained by the small sample of 7 total participants and 10 trials in each of the skating conditions. For the inline skating tasks, they had a single participant perform the same circuit ten times. Therefore, it would be reasonable to believe that the model was well trained in classifying tasks from that same participant and could explain the high F1 score for that dataset. Although this may seem like a good score, it is likely not generalizable to other players who may demonstrate different movement patterns in performing the same tasks. Having a larger sample of players would likely lower the F1 score. In the on-ice skating tasks, there were 6 different players who performed the same circuit a total of 10 times (1-3 times each). This dataset had a greater variability of participants which could explain the lower F1 score but could be more representative of what we could expect to find in future studies. The total sample size for a machine learning model in this study is very small, therefore more research with larger samples would be required in order to confirm their results.

There are very few other studies in ice hockey looking at task recognition from acceleration data; however, studies in sports with similar stride movement patterns such as cross-country skiing have been published. For example, Jang et al. (2018) used a convolutional neural

network to classify classical and skating styles of cross-country skiing. They used a 17 sensor IMU system and compared accuracy of different configurations. They compared whole-body, upper body, lower body, sports biomechanics configuration (pelvis, two wrists and two feet) and pelvis only. They found that using the sports biomechanics configuration, they were able to obtain the highest accuracy (91.2%) when classifying skiing sub-technique on flat and natural surfaces.

Similarly, Sakurai, Fujita, and Ishige (2016) used sensor placement on both feet and both wrists to classify skating ski style sub-techniques using a decision tree classification model. This 4-sensor configuration and decision tree model accurately classified 94.8% of skiing cycles. Finally, Rindal, Seeberg, Tjonns, Haugnes, and Sandbakk (2017) used 2 sensors, one on the chest and one on the wrist, to classify 6 classical skiing styles. They implemented a neural network with their dataset and accurately classified 93.9% of strides.

One of the more evident differences between cross-country skiing and ice skating is arm motions. In skiing, athletes use different pole strokes for different techniques (Sakurai et al., 2016). Thus, having one sensor on the wrist can be beneficial in differentiating between skiing styles. Comparatively, ice skating uses very similar arm motions whether the athlete is performing a start or skating full speed. Jang et al. (2018) found that the accuracy of a k-nearest neighbor and deep learning models ranged between 64.6 and 84.4% accuracy using 7 lower body sensors and no wrist sensors. This range of accuracy may be more similar to the results one would find when classifying different skating tasks considering the motions of the lower body are more similar between skating and skiing than the arm motion.

Classifying skating tasks using kinematic data seems feasible considering previous literature demonstrating unique kinematic profiles of different skating tasks. As previously mentioned, segment movements are produced by periodic segments accelerations, data that are

easily accessible from commercial accelerometers that are commonly used for player tracking. With more and more professional sports teams collecting acceleration data from IMU systems, implementing a ML model using this data could lead to more in-depth analysis of player movements on the ice. Therefore, a study is needed to determine the feasibility of using acceleration data to classify different on-ice skating and shooting tasks prior to implementing such methods and to progress our knowledge of player tracking in hockey.

1.5 Objectives & Hypothesis

The primary objective of this study was to compare the accuracy of a Support Vector Machine (SVM) and a Random Forrest Classifier (RF) model using Machine Learning (ML) in classifying four different hockey tasks using individual segment Centre of Mass (CoM) acceleration data collected from passive motion capture systems. These two models were selected as they are known to be two of the more common algorithms used in sport and gait activity classification (Cust, Sweeting, Ball, & Robertson, 2019; Figueiredo, Santos, & Moreno, 2018; Halilaj et al., 2018).

If teams and coaches are to use ML to assist in task classification, it would not be feasible to have players wear numerous sensors while participating in the sport as it could impede performance. Thus, minimizing the number of sensors as much as possible would allow players to move naturally on the ice. Previous research in locomotion activity classification in sport has used sensor locations including foot, shank, thigh, pelvis and/or trunk (Clermont, Benson, Osis, Kobsar, & Ferber, 2019; Dixon et al., 2019; Hardegger et al., 2015; Jang et al., 2018). Thus, a secondary objective of this study was to compare the performance of individual segment data input into each of the SVM and RF models to determine which segment(s) sensors had a great

influence on model performance. The purpose of comparing individual segment inputs was to determine the optimal combination and number of segment data inputs to achieve the greatest accuracy in task classification. Trunk and lower body segments were used for this study given their evident gross movement involvement in skating locomotion (Buckeridge et al., 2015; Budarick et al., 2018; Renaud et al., 2017; Shell et al., 2017).

The study's specific hypothesis were:

- An SVM and RF model will achieve an F1 score greater than 80% in correct skating task identification.
- Lower extremity segments (foot, shank, thigh) will outperform axial skeleton segments (trunk & pelvis) in terms of correct skating task identification.

CHAPTER 2: METHODS

2.1 Participants

Skating motion capture data from 75 unique participants performing four different hockey tasks (starts, strides, stop & go and wrist shot) were included in this study from seven separate datasets that were previously collected for different research projects (Table 1). Anonymized data were included from both male and female participants, varying in playing positions from forwards and defence as well as from high to low calibre. Note our intent was to include hockey players of varied skating proficiency to improve our models' generalizability. All participants were free of lower body injuries. Anonymized data files from prior studies were used.

Table 1 Participant and task characteristics (See Appendix A-D for task visual representations).

	Participants	Descriptive Statistics	Task Description
Dataset 1 – Hallihan (2018)	<ul style="list-style-type: none"> 9 high calibre males 11 high calibre females 	<p>Male</p> <ul style="list-style-type: none"> Age – 24.1 +/- 3.8 yrs Height – 1.80+/- 0.09m Weight – 85.4+/- 8.5kg Experience – 19.2+/- 3.42yrs <p>Female</p> <ul style="list-style-type: none"> Age – 19.6+/-1.3 yrs Height – 1.71+/-0.07m Weight – 71.3+/-9.9kg Experience – 12.8 +/- 1.9yrs 	Stop & Go: Parallel standing cross over start, skate forward, perform 2-foot side parallel stop, cross over again and skate back to start from blue line to blue line
Dataset 2 – Budarick et al. (2018)	<ul style="list-style-type: none"> 9 high calibre males 10 high calibre females 	<p>Male</p> <ul style="list-style-type: none"> Age - 22+/-1yrs Height – 1.81+/-0.08m Weight – 81.5+/-8.4kg Experience – 16+/-2yrs <p>Female</p> <ul style="list-style-type: none"> Age - 21+/-1yr Height – 1.72+/-0.07m Weight – 71.2+/-10.4kg Experience – 14+/-1yrs 	Stride: Start on goal line and skate through until far blue line. Data collected from blue line to blue line
Dataset 3 – Shell et al. (2017)	<ul style="list-style-type: none"> 9 high calibre males 10 high calibre females 	<p>Male</p> <ul style="list-style-type: none"> Age - 22+/-1yrs Height – 1.81+/-0.08m Weight – 81.5+/-8.4kg Experience – 16+/-2yrs <p>Female</p> <ul style="list-style-type: none"> Age - 21+/-1yr Height – 1.72+/-0.07m Weight – 71.2+/-10.4kg Experience – 14+/-1yrs 	Start: Forward start from stand still; blue line to blue line capturing 7 steps
Dataset 4 – Renaud et al. (2017)	<ul style="list-style-type: none"> 8 high calibre males 8 low calibre males 	<p>High Calibre</p> <ul style="list-style-type: none"> Age – 24.7+/-3.1yrs Height – 184.2+/-6.4cm Weight – 87.1+/-6.0kg Experience – 19.7+/-3.9yrs <p>Low Calibre</p> <ul style="list-style-type: none"> Age – 23.9+/-3.1yrs Height – 179.4+/-3.4cm Weight – 81.3+/-8.4kg Experience – 9+/-6yrs 	Start: Parallel start from stand still, first 4 strides collected
Dataset 5 – Unpublished data from Renaud et al. (2017)	<ul style="list-style-type: none"> 6 high calibre males 8 low calibre males 	<p>High Calibre</p> <ul style="list-style-type: none"> Age – 24.7+/-3.1yrs Height – 184.2+/-6.4cm Weight – 87.1+/-6.0kg Experience – 19.7+/-3.9yrs <p>Low Calibre</p> <ul style="list-style-type: none"> Age – 23.9+/-3.1yrs Height – 179.4+/-3.4cm Weight – 81.3+/-8.4kg Experience – 9+/-6yrs 	Stride: Start on goal line and skate through until near blue line. Data collected from top of circle to blue line (7m)
Dataset 6 – McPhee (2018)	<ul style="list-style-type: none"> 9 high calibre males 	<ul style="list-style-type: none"> Age – 24.11(3.54)yrs Height – 1.80(0.07)m Weight – 85.4(7.97)kg Experience – 19.8(3.42)yrs 	Start: Forward facing start from stand still for 15m, blue line to blue line
Dataset 7 –Robbins, Renaud, MacInnis, and Pearsall (2020)	<ul style="list-style-type: none"> 10 high calibre males 10 low calibre males 	<p>Elite</p> <ul style="list-style-type: none"> Age – 26+/-5yrs Height – 1.82+/-0.04m Weight – 86.70+/-5.44kg <p>Recreational</p> <ul style="list-style-type: none"> Age – 26+/-5yrs Height – 1.81+/-0.05m Weight – 85.75+/-8.74kg 	<p>Wrist Shot:</p> <p>1) Stationary wrist shots from 9m in front of net</p> <p>2) Skating wrist shots released at approximately 9m from net</p>

2.2 Data Collection

All data were collected using multiple infrared cameras on the arena ice surface (Vicon Motion Systems Ltd., Oxford, UK). Movements within the skating space were calibrated before each skating session. Residual error were less than 0.2 mm per camera. The capture rate of kinematic data were 240Hz for all datasets. Participants wore a tight-fitting suit (OptiTrack Motion Capture Suit, NaturalPoint Inc. Corvallis OR, United States) upon which 14mm reflective markers were attached. See Table 2 and Table 3 for individual dataset collection and processing details.

Table 2 Motion capture camera and marker set up.

	Vicon Cameras	Capture Area (volume)	Reflective Markers
Dataset 1 – Hallihan (2018)	<ul style="list-style-type: none"> • 8 T10S • 2 T40S • 8 T20 • Total = 18 cameras 	3m wide x 15m long x 2m high	51
Dataset 2 – Budarick et al. (2018)	<ul style="list-style-type: none"> • 8 T10S • 2 T40S • 8 T20 • Total = 18 cameras 	3m wide x 15m long x 2m high	67
Dataset 3 – Shell et al. (2017)	<ul style="list-style-type: none"> • 8 T10S • 2 T40S • 8 T20 • Total = 18 cameras 	3m wide x 15m long x 2m high	81
Dataset 4 – Renaud et al. (2017)	<ul style="list-style-type: none"> • 8 MX3 • 2 T40S • Total = 10 	3m wide x 6.5m long x 1.5m high	24
Dataset 5 – Unpublished data from Renaud et al. (2017)	<ul style="list-style-type: none"> • 8 MX3 • 2 T40S • Total = 10 	3m wide x 6.5m long x 1.5m high	24
Dataset 6 – McPhee (2018)	<ul style="list-style-type: none"> • 8 T10S • 4 Vantage V5 • 4 Vero • 2 T40S • Total = 18 	3m wide x 15m long x 2m high	48
Dataset 7 – Robbins et al. (2020)	<ul style="list-style-type: none"> • 8 T10S • 2 T40S • 4 Vantage V5 • Total = 14 	9m wide x 9m long x 2 m high	79

Table 3 Data processing criteria.

	Gap filling	Filter	Data Collection Events
Dataset 1 – Hallihan (2018)	<ul style="list-style-type: none"> • Vicon Nexus 2.5 software • Rigid body fill and pattern fill 	<ul style="list-style-type: none"> • 4th order Butterworth filter • Cut-off frequency of 8Hz 	<ul style="list-style-type: none"> • S1OFF pre-stop to S5OFF post-stop
Dataset 2 – Budarick et al. (2018)	<ul style="list-style-type: none"> • Vicon Nexus 2.1.1 • Rigid-body fill and Woltring fill 	<ul style="list-style-type: none"> • 4th order low pass Butterworth filter • Cut-off frequency of 8Hz 	<ul style="list-style-type: none"> • S1ON to S3OFF
Dataset 3 – Shell et al. (2017)	<ul style="list-style-type: none"> • Vicon Nexus 2.1.1 • Rigid body fill and Woltring fill 	<ul style="list-style-type: none"> • 4th order low pass Butterworth filter • Cut-off frequency of 8Hz 	<ul style="list-style-type: none"> • S1OFF to S7ON
Dataset 4 – Renaud et al. (2017)	<ul style="list-style-type: none"> • Vicon IQ 2.5 • Spline fill 	<ul style="list-style-type: none"> • 4th order low pass Butterworth filter • Cut-off frequency of 6Hz 	<ul style="list-style-type: none"> • S1OFF to S4ON
Dataset 5 – Unpublished data from Renaud et al. (2017)	<ul style="list-style-type: none"> • Vicon IQ 2.5 • Spline fill 	<ul style="list-style-type: none"> • 4th order low pass Butterworth filter • Cut-off frequency of 6Hz 	<ul style="list-style-type: none"> • S1ON to S4OFF
Dataset 6 – McPhee (2018)	<ul style="list-style-type: none"> • Vicon Nexus 2.2.5 software • Rigid-body fill and pattern fill 	<ul style="list-style-type: none"> • 4th order low pass Butterworth filter • Cut-off frequency of 8Hz 	<ul style="list-style-type: none"> • S1OFF to S7ON
Dataset 7 – Robbins et al. (2020)	<ul style="list-style-type: none"> • Vicon Nexus 2.1.1 • Rigid body fill and Woltring fill 	<ul style="list-style-type: none"> • 4th order, recursive, low pass Butterworth filter • Cut-off frequency of 25Hz 	<ul style="list-style-type: none"> • S1OFF to 10 frames after puck release

For each study, marker data were input to Visual3D (Version 5.01.23, C-Motion, Germantown, Maryland, USA) from which kinematic measures of body markers, segments and joints can be calculated. These data were then exported into MatLab (Mathworks, Natick, Massachussettes, U.S.A) to be analyze further using custom scripts based on the biomechZoo toolbox (Dixon, Loh, Michaud-Paquette, & Pearsall, 2017). Time-series linear acceleration in X, Y and Z directions were derived from position data of the trunk, pelvis, thigh, shank and foot (skate) from each trial and were exported as a .csv file.

2.3 Machine Learning (ML) Models

SVM and RF models are both supervised learning methods, meaning the training set is labeled with the tasks prior to training the model. The SVM model uses optimal hyperplanes to separate classes by finding the largest gap between data points of different classes. Data points from a new data set are classified based on which side they fall on in relation to the most optimal hyperplane (Figure 2) (Garreta & Moncecchi, 2013). RF models use multiple layers of binary

decision trees with randomized explanatory variables to develop a framework for making classification decisions (Figure 3). New data that is then input into the model is passed through the same framework to reach a classification decision (Genuer, Poggi, & Tuleau, 2008). These models were implemented using the Scikit-Learn module (Pedregosa et al., 2011) in Python (Python Software Foundation, <https://www.python.org/>).

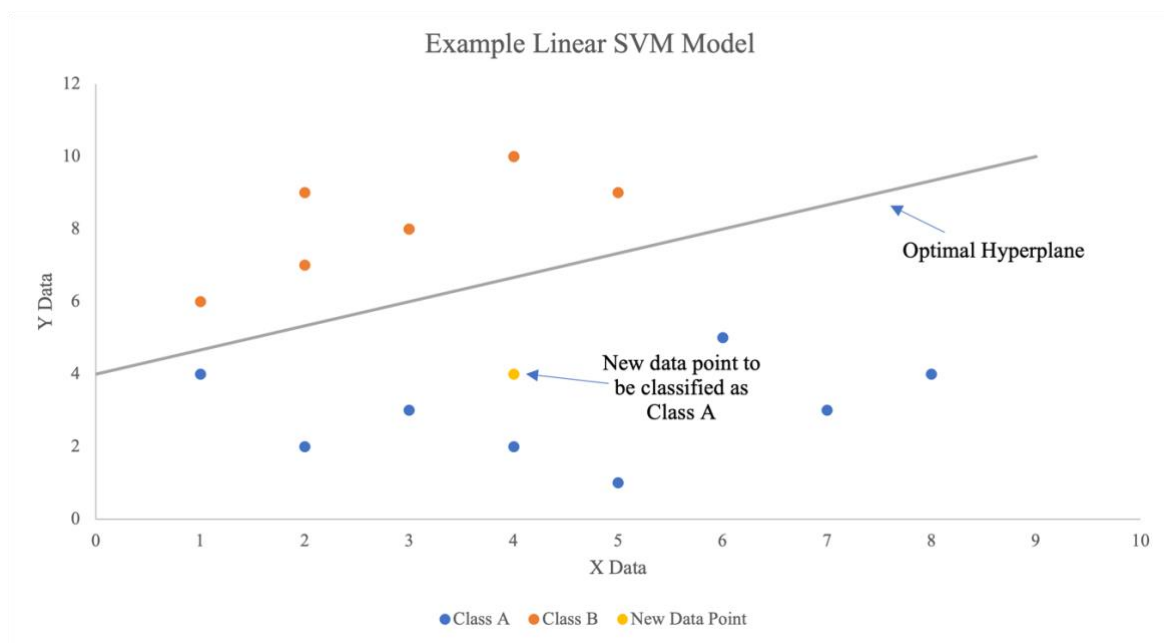


Figure 2 Example of a linear SVM ML model (Garreta & Moncecchi, 2013)

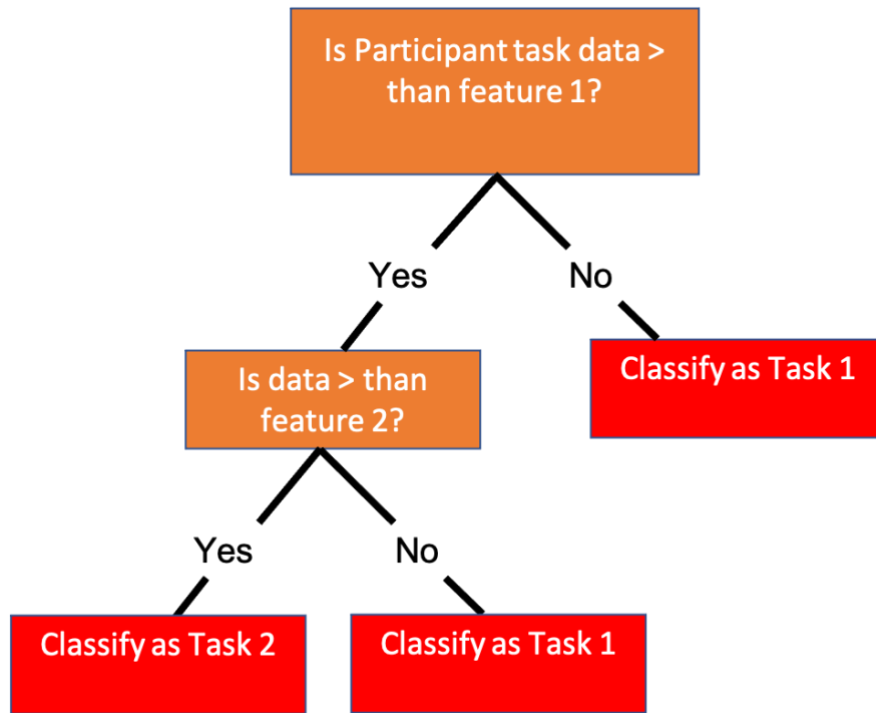


Figure 3 Simplified example of a decision tree ML model (Genuer et al., 2008).

2.4 Feature engineering

With ML models, features are data characteristics input into the model to discriminate different data patterns. For each trial, segment centre of gravity acceleration outputs were used to create features in the X, Y and Z directions for each individual segment. A total of 224 features (8 markers x 3 directions x 9 features = 216 features + 8 markers x 1 non-directional feature = 224 features) were extracted consisting of statistical features, time domain analysis features and frequency domain analysis features (Clermont et al., 2019; Srinivasan, Eswaran, & Sriraam, 2007). When features were split into their respective datasets, the bilateral foot, shank and thigh segment datasets were combined for 56 features (S1 and S2) while the pelvis and trunk had 28. Features were formed in Matlab and exported as a .csv file. Each feature was then scaled from 0 to 1 based on the minimum and maximum values for each trial. See Table 4 for all features.

Table 4 Features engineered and input into ML model.

Features			
Statistical Features	Mean	Standard Deviation	Maximum
	Minimum	Skewness	Kurtosis
Time domain analysis	Root Mean Square	Resultant Root Mean Square	Entropy
Frequency domain analysis	Mean Power Frequency		

2.5 Model Segment Configuration

Six SVM models were created for the current study: a foot segment model, a shank segment model, a thigh segment model, a pelvis segment model, a trunk segment model and a model with all segments. The trunk segment model excluded 2 datasets: one start task (Renaud et al., 2017) and one stride task (unpublished data from Renaud et al. (2017)) as both datasets did not collect trunk segment data.

2.6 Model Performance Analysis

The model was trained using a standard consumer computer. Training a ML model consists of splitting the data into a training and test set. The train dataset was input into the model and allowed it to become familiar with (e.g. to train) patterns in the data. The test set was then input into the model where it will make predictions based on its knowledge of patterns from the train input. A 75/25 inter-subject splitting procedure was performed on the data to select training data (56 participants) and test data (19 participants) for all datasets, except for the two datasets without trunk segment data which were split to obtain training data (45 participants) and test data (14 participants). Grid search was performed for ‘C’ and ‘kernel’ of the SVM model to determine the optimal parameters by finding the accuracy of the model using different

combinations of model parameters (Garreta & Moncecchi, 2013). The ‘C’ attribute of the SVM model is a measure of regularization, also known as a “soft margin” (Hastie, Rosset, Tibshirani, & Zhu, 2004). In most situations, a single line will not be able to separate two classes of data to form an optimal hyperplane and there will be some overlap of data points. Regularization provides a buffer area where data points can be on the wrong side of the hyperplane and ‘C’ inversely controls the amount of overlap (large ‘C’ defines a small margin) (Hastie et al., 2004). The attribute ‘kernel’ in the SVM model defines the shape of the hyperplane, being linear or nonlinear (e.g. RBF kernel) (Garreta & Moncecchi, 2013). Performance of the default parameters for the RF model were deemed good; therefore, default parameters were used for the RF model and ‘C’ of 1.0 with a linear kernel was used for the SVM model to allow for determination of feature weights in influencing task classification using the coefficients attribute of this particular model. A 10-fold cross validation technique was used on each segment dataset to validate model accuracy and mitigate overfitting. This technique resamples the data with each iteration of training the model, using different combinations of test/train splits to reduce the risk of achieving a score by chance (Wong & Yeh, 2020). Model performance was evaluated using test data set. The mean value of the ten cross validation iterations for each dataset were used to calculate the following metrics and evaluate model performance: F1 score (Equation 1), precision (Equation 2), recall (Equation 3), and specificity (Equation 4).

(1)

$$F1 = \frac{2 \times (\text{Precision} \times \text{Recall})}{\text{Precision} + \text{Recall}}$$

(2)

$$\text{Precision} = \frac{\text{True Positive}}{\text{True Positive} + \text{False Positive}}$$

(3)

$$\text{Recall} = \frac{\text{True Positive}}{\text{True Positive} + \text{False Negative}}$$

(4)

$$\text{Specificity} = \frac{\text{True Negative}}{\text{True Negative} + \text{False Positive}}$$

F1 score was selected over model accuracy as the main performance metric because the sample of tasks was imbalanced with a greater number skating starts than other tasks. In this situation, F1 score were a better measure of the model performance. Precision was calculated as a measure of the model's ability to identify the correct task. Recall and specificity were calculated as a measure of the model's ability to differentiate correct from not correct tasks, respectively. In other words, recall and specificity were used to measure the model's ability to classify tasks which were in fact the correct task as well as the model's ability to not classify tasks that were not the correct task. A 4x4 confusion matrix was also created for each iteration of each segment model to compare model performances. See Figure 3 for a visual of the machine learning process. Finally, feature importances were obtained using Gini importance ('feature_importances_' attribute of the RF model in Scikit-Learn module) (Zhang & Ma, 2012) and weight vector derivatives ('coeff_' attribute of the SVM model in Scikit-Learn module)

(Rakotomamonjy, 2003) to determine which features had the greatest relevance on model performance.

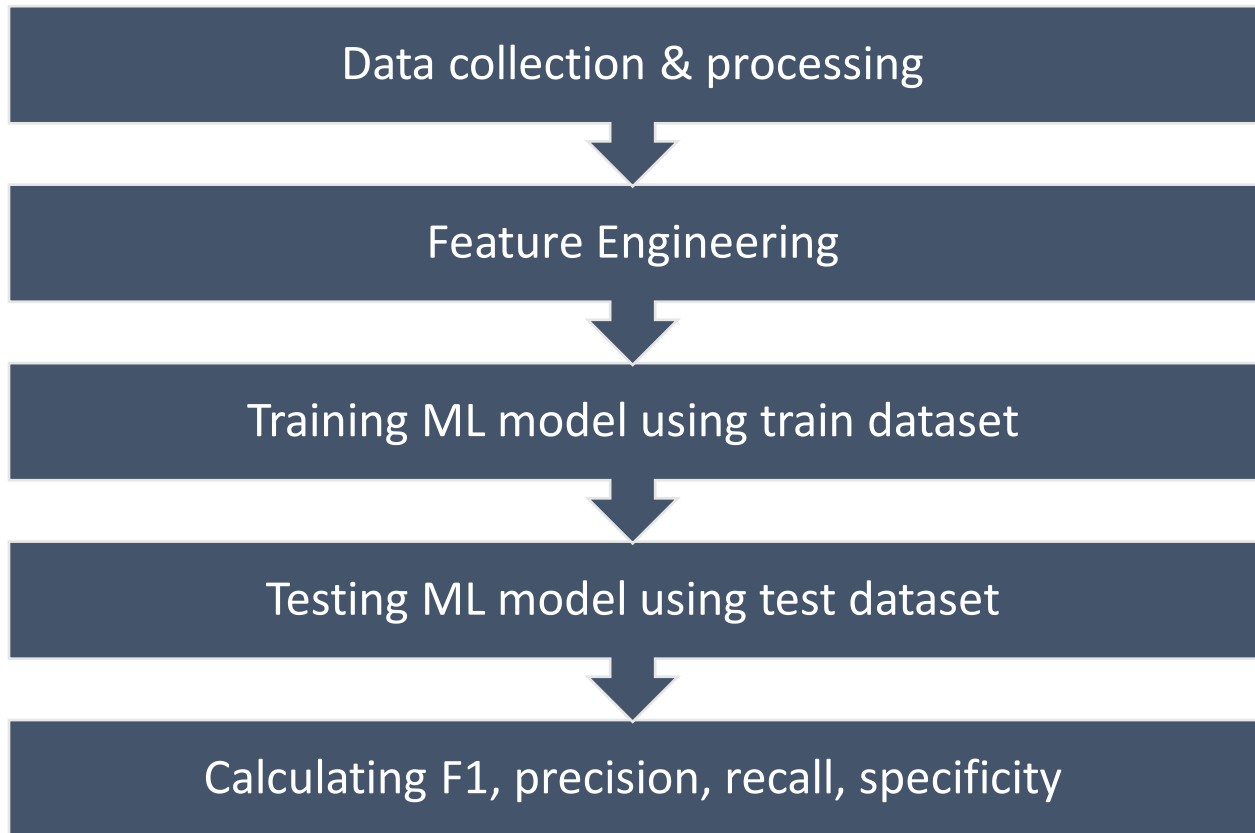


Figure 4 A simplified flow chart demonstrating the step-by-step process of evaluating a ML model performance (adapted from Mannini and Sabatini (2010)).

CHAPTER 3: RESULTS

3.1 Model and Segment Performance

The SVM model had strong performances in five of the six segment configurations while the Random Forrest model performed well with all segment configurations (Table 5, Table 6 and Figures 5). F1 score is the harmonic mean of precision and recall; hence, a large F1 score demonstrates a high precision and recall. In general, most individual sensors (e.g. linear accelerations of segment center of mass) demonstrated high performances measured in all F1, Precision, Recall, and Specificity scores, with most scores ranging from 92.1 to 99.2. Of note, the trunk segment performed least well in the SVM with scores ranging from 69.1 to 96.2, yet in the Random Forrest model the trunk segment scores were some of the highest (96.6 to 99.3). Also of note, the score of All combined sensors did not necessarily yield higher scores than individual sensors.

Sensor	SVM			
	F1 Score	Precision	Recall	Specificity
All	96.2 (5.2)	96.0 (5.5)	95.9 (5.2)	98.6 (1.7)
Trunk	69.1 (5.9)	67.1 (6.4)	88.6 (7.8)	96.2 (2.6)
Thigh	92.1 (5.1)	93.5 (4.1)	93.0 (5.0)	97.7 (1.7)
Pelvis	97.0 (3.0)	96.8 (3.3)	96.8 (3.7)	98.9 (1.2)
Foot	97.1 (2.8)	97.2 (3.0)	96.9 (3.4)	99.0 (1.1)
Shank	96.8 (3.2)	97.1 (3.5)	96.8 (3.9)	98.9 (1.3)

***Table 5** Mean percentage (standard deviation) of model performance for the six segment configurations. The “All” sensor configuration combines input from the five individual segments. Highest average scores are in bold.*

Sensor	Random Forrest			
	F1 Score	Precision	Recall	Specificity
All	96.6 (5.1)	96.5 (6.1)	96.6 (5.5)	98.9 (1.8)
Trunk	96.6 (2.4)	98.9 (0.7)	98.0 (1.5)	99.3 (0.5)
Thigh	97.1 (5.1)	97.2 (3.6)	96.9 (3.9)	99.0 (1.3)
Pelvis	96.7 (2.5)	97.2 (2.4)	96.9 (2.7)	99.0 (0.9)
Foot	97.6 (2.2)	98.0 (2.2)	97.5 (2.7)	99.2 (0.9)
Shank	96.3 (3.4)	97.0 (3.4)	96.4 (4.0)	98.8 (1.3)

Table 6 Mean percentage (standard deviation) of model performance for the six segment configurations. The “All” segment configuration combines input from the five individual segments. Highest average scores are in bold.

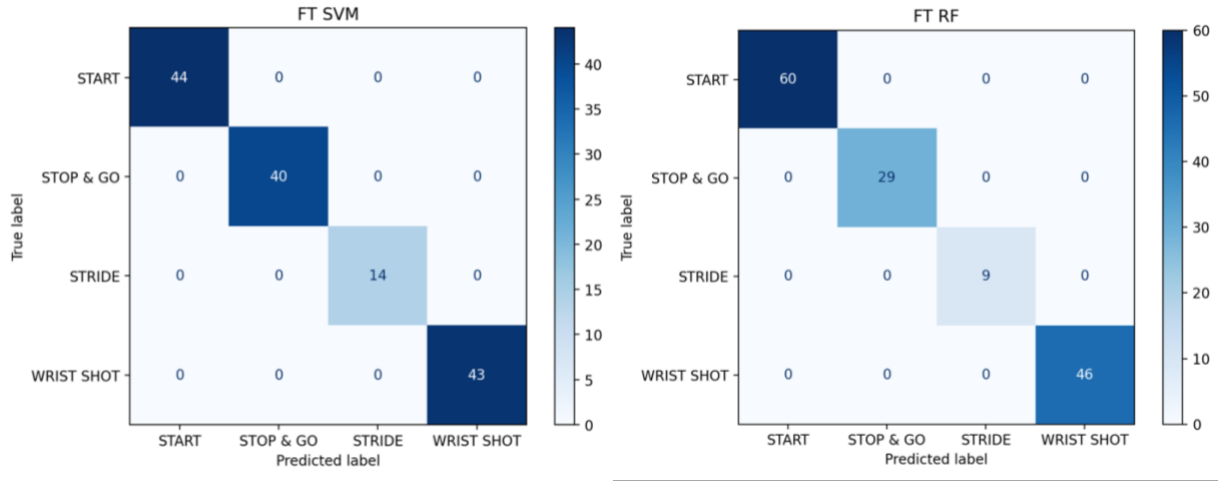


Figure 5 Example confusion matrices of the top performing foot segment from the 10-fold cross validation SVM and RF models. **FT** = Foot segment (See Appendix E-G for top, moderate and poor performing models from all segment models).

3.3 Feature Importances

Feature importances were calculated for each model, demonstrating the relevance of each feature in differentiating the tasks (Rakotomamonjy, 2003; Zhang & Ma, 2012). The top 10 ranked features for each segment configuration of the RF model can be seen in Figure 7, while the top 10 features for each segment configuration of the SVM model can be seen in Figure 8. Skewness was an important factor in differentiating tasks using axial skeleton data (trunk and pelvis) (Figures 7a, b, c, d, f and Figures 8a, b, c, d, e, f), which are common estimates of total body CoM, as well as in differentiating tasks using all segments. Lower body segment data have had a greater variety of important features between segments.

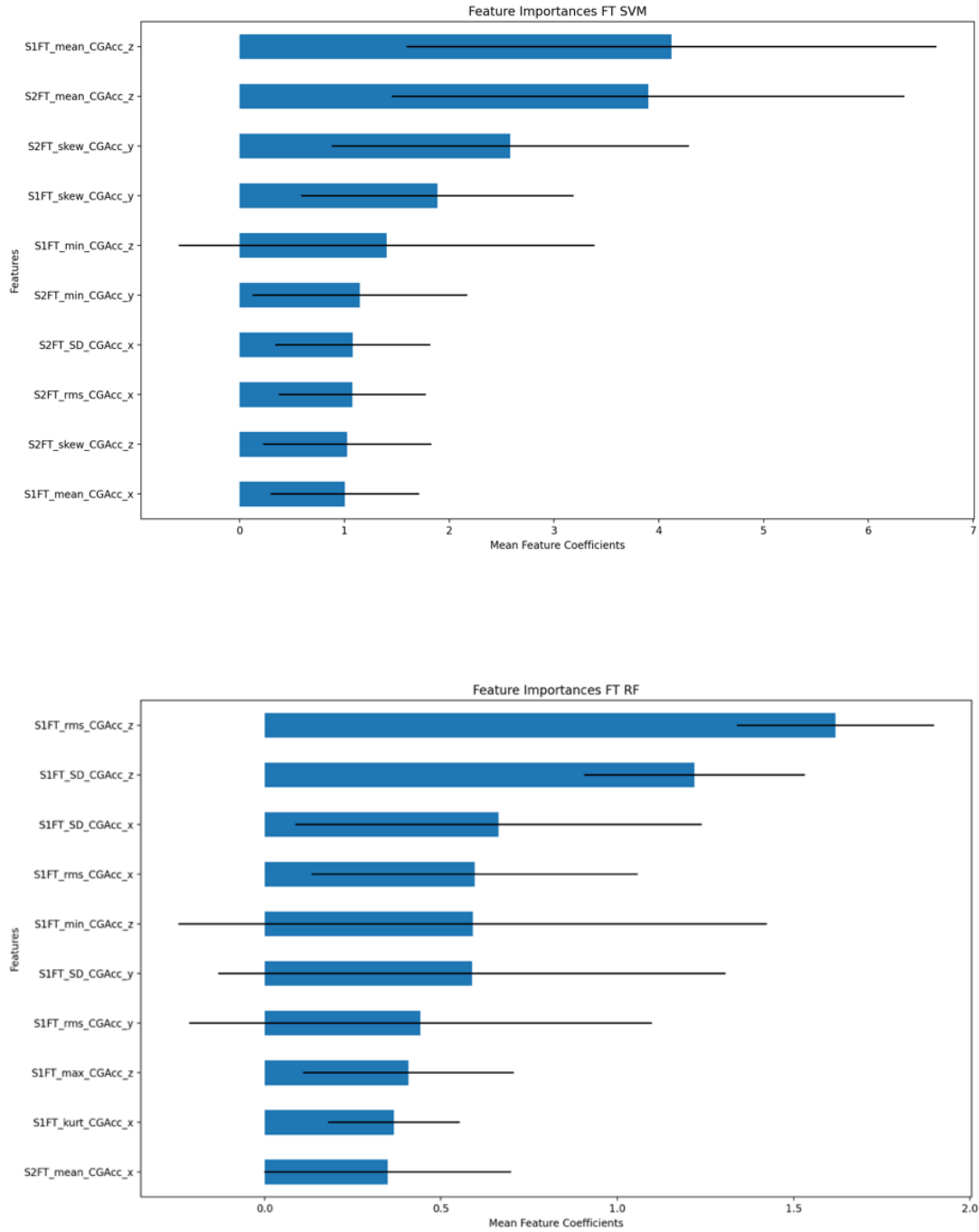


Figure 6 Top 10 feature importances (mean and standard deviation) of the SVM and RF models for the top performing foot segment. **S1** = Side of step 1, **S2** = Side of step 2, **FT** = Foot segment, **skew** = Skewness, **kurt** = Kurtosis, **SD** = Standard Deviation, **rms** = Root Mean Square, **min** = Minimum, **CGAcc_x** = Segment center of gravity acceleration in the x direction, **CGAcc_y** = Segment center of gravity acceleration in the y direction, **CGAcc_z** = Segment center of gravity acceleration in the z direction (See Appendix H and I for feature importances of other segment models).

CHAPTER 4: DISCUSSION

The purpose of this study was to evaluate the ability of ML algorithms to classify different on-ice hockey tasks. The main objective was to compare the performance of an SVM model and a RF model in classifying four different hockey tasks. A secondary objective was to evaluate the performance of individual segment acceleration data in the classification of the same four hockey tasks.

One of the strengths of this study was the sample size. Previous work by Hardegger et al. (2015) had only one inline skater and six on-ice skaters perform different skating tasks, for a total of seven participants. Small sample sizes reduce the generalizability of the ML model. Large sample sizes are needed to train a ML model to identify specific features within time-series kinematic data input that are related to differences between tasks and to be generalizable e.g. the results of a study apply to individuals and circumstances beyond those skaters studied. The larger sample size of 75 participants in the current study provided substantial variety of skating patterns that made accurate task classification difficult; however, this afforded it greater generalizability to identify tasks. The results show that both ML models performed relatively well with a larger sample, with F1 scores (combined recall and precision) ranging from 69.1 to 97.1% using the SVM model and 96.3 to 97.6% using the RF model. These results suggest that the models could be used with a greater variety of skating patterns including backwards skating, crossovers and pivots.

4.1 Model Performance

The SVM model is a classification model that finds the optimal hyperplane to separate classes and makes predictions based on which side of the hyperplane that new instances of skating data set fall (Garreta & Moncecchi, 2013). Comparatively, the RF model uses binary

decision trees to form a task classification framework (Genuer et al., 2008). The results of our study partially support (i.e. 4/5 segments scored >90% in SVM model, trunk scored 69%) our hypothesis that both SVM and RF models would be able to predict skating tasks with an F1 score of 80%. Based on the results from Hardegger et al. (2015) who achieved an F1 score of 65% using one ice hockey participant, it was our belief that the larger sample size of the current study would demonstrate higher accuracy, therefore hypothesising an F1 score of 80%. Our results showed that the individual segments as well as all segments combined using the RF model achieved F1 scores over 90% while four of five segments as well as all segments combined using the SVM model achieved F1 scores over 90% with the trunk being the only segment not to reach 90%.

Considering the architecture of the models, this suggests that the trunk acceleration in the four tasks is too similar for the SVM model to differentiate. If the data points are similar between tasks, there is a greater chance that a data point of one class would fall on the side of another class. The lower precision of the trunk segment with the SVM model would suggest that it had issues predicting the correct task whereas the higher specificity suggests the model was better able to predict negative classes. In other words, the model had difficulty predicting which class the new data point belonged to but not which class it did not belong to. Comparatively, the RF model uses multiple decision trees to determine the classification of the test data. This model performs multiple predictions and the most common amongst the trees is the final class prediction (Garreta & Moncecchi, 2013). The trunk segment performed well with the RF model, which would suggest that the RF model was better at differentiating the tasks using trunk acceleration.

If we consider the trunk segment to estimate the body's CoM, previous research has shown small yet significant differences in forward acceleration skating starts and skating strides (Budarick et al., 2018). However, it is possible that the features used in the present study were

not appropriate for identifying these small differences. For example, research by Clermont et al. (2019) to classify male and female competitive and recreational runners found a 69% classification accuracy using data from the lumbar spine level and an SVM model. They also discovered the more dominant features of their models were RMS, step/stride regularity and step/stride variability. Although the current study did use features related to RMS, features related to step/stride regularity and variability were not used. Therefore, it is possible that a different set of features other than accelerations could result in higher performance of the trunk segment with the SVM model.

Although SVM models are most used and often perform better than other models in activity classifications (Cust et al., 2019), this was not the case in the current study. The RF classifier performed better than the SVM classifier with all six segment models suggesting that RF may be a superior model for classification of ice hockey tasks.

4.2 Segment Performances

SVM models of four of the five segments and all segments combined obtained F1 scores over 90%. These segments were the foot, shank, pelvis, and all segments combined. All RF models obtained F1 scores over 90%. Previous research in the classification of activity has shown that sensor placement does in fact matter in classification accuracy. For example, Janidarmian, Roshan Fekr, Radecka, and Zilic (2017) showed that in classifying standing, walking, sitting, laying, stair ascent/descent and jogging, the thigh, chest and lower leg had the highest accuracy of classification. Comparatively, both Panebianco, Bisi, Stagni, and Fantozzi (2018) and Vahdatpour, Amini, and Sarrafzadeh (2011) demonstrated that the foot and shank were preferred sensor locations for high accuracy classifications of gait. These studies suggest that sensor accuracy could be task specific.

The highest F1 score in the current study was of the foot (left and right) in both SVM and RF models, in agreement with Panebianco et al. (2018) and Vahdatpour et al. (2011) findings. This suggests that foot linear acceleration data is the best for classifying ice hockey starts, strides, stop & go and shots. Budarick et al. (2018) reported that the run-to-glide forward skating transition distinctly changes from unimodal to bimodal forward accelerations as well as from negative to forward deceleration intervals (Pearsall et al., 2000; Renaud et al., 2017). This could explain why the most distal segments, the feet, demonstrated the greatest relationship to skating tasks and thus were more accurate classification.

4.3 Feature Importances

Feature importances tell us which features were the most relevant in making classification predictions. Skewness appeared to be the most relevant feature for the axial skeleton segment models (i.e. trunk and pelvis), whereas lower body segments had more variation in relevant features. For example, from Budarick et al. (2018) skating start data, initial CoM accelerations were high for the first five strides then dropped and plateaued during latter steady state strides. This could explain why skewness was a highly relevant feature in the task selection; that is, skating start trials consisted of grouped data early on in the trial which would have leveled off later as the player reaches full stride. As another example, the stop & go tasks had two instances of skewed data during the trial: once at the start as the player accelerates and again to accelerate after the full stop. In contrast, we would expect to have less skewness (i.e. less acceleration variance, lower stride frequency) in steady-state skating strides, including the skating approach to shooting trials.

4.4 Misclassifications

Despite the above, the confusion matrices showed greater misclassification rates between strides, starts and stop & go tasks. This may have been due to similarities e.g. all tasks included skating starts as part of the whole task. As well, misclassifications may be attributed to the different datasets used in the sample. For example, Shell et al. (2017) and Renaud et al. (2017) start tasks had different distances i.e. participants in Shell et al. (2017) study may have shown both stride characteristics of the skating start and steady-state skating that may have led to task misclassification.

4.5 Limitations

The current study has several limitations. First, although Vicon is known as one of the “gold standard” for 3D motion capture systems, the majority of recent research in sport task recognition adopt body worn IMU acceleration data. The latter method is more practical in the sport setting, due to the much larger potential capture volume, thus making the information more transferable and externally valid. However, in this study the McGill Ice Hockey Research Group’s extensive skating mocap database was adopted, using segment derived acceleration data to mimic the acceleration data collected from IMU systems. The quality of mocap segment derived acceleration data may vary from accelerometer data from IMU. Previous studies comparing IMU systems to camera-based motion capture have shown differences in joint angles, acceleration and velocity calculations which may be attributed to integration drift (Schepers, Giuberti, & Bellusci, 2018; Zhao, 2018). Thus, with higher quality data collected in this study compared to what would be collected using IMUs, the current results may be an overestimation of what would be achieved using IMU systems on the ice. Nevertheless, the high classification rates of our ML models using mocap data lead us to believe high classification rates could also be achieved using IMU systems.

Second, the datasets consisted of distinct and delimited tasks and trials. Correspondingly, this led to the model learning of four discrete tasks. In contrast, ice hockey players will perform many different tasks in sequence and in varying order while on the ice during the game. It is unknown how well these models will perform given data input of players skating transitions between many different tasks. Hence, further research is necessary to determine the performance of machine learning models during sequential tasks. Additionally, there was only one skating shot task included in the dataset. It would also be necessary to evaluate the performance of a model on other concurrent skating-shot and skating-passing tasks to further understand the full potential to classify all hockey tasks.

Another limitation of the study was that trials were not time-normalized so trial time length could have impacted model predictions. For example, the stop & go task duration was almost twice as long than the other tasks, therefore creating time-dependant features, like the mean linear acceleration, could lead to erroneous larger task classification values.

Finally, the sample consisted largely of high calibre male players, bringing into question the generalizability of such models in low calibre and in female hockey players. Previous research in ice hockey has identified kinematic differences in skating between high calibre and low calibre players as well as males and females (Budarick et al., 2018; Renaud et al., 2017; Shell et al., 2017). Thus, future studies should focus on increasing the sample size, using more female hockey players, and attempting to classify skill level based on kinematic data.

CHAPTER 5: CONCLUSION

Ice hockey is often said to be as the fastest game on earth. With high speeds, it is challenging to identify and classify in-game tasks. Previous studies have used time consuming and low accuracy methods to track and classify on-ice tasks (Bracko et al., 1998; Montgomery et al., 2004); however, with the explosion in sports analytics, the amount and types of data currently being collected by professional hockey teams is over whelming. To make sense of this data, machine learning techniques demonstrate the potential for more efficient and accurate tracking on-ice tasks.

This study compared SVM and RF machine learning algorithms in the classification of four on-ice tasks (skating start, skating stride, stop & go and wrist shot) using trunk, pelvis, thigh, shank and foot linear accelerations. The RF model had superior performance compared to the SVM model (with classification scores ranging from 69.1-97.1% and 96.3-97.6%, respectively) while the foot segment provided the greatest task identification accuracy compared to the other segments.

This study demonstrates the feasibility of using body segment acceleration input to identify specific ice hockey tasks using machine learning. Given the accuracy of the machine learning models in this study using motion capture acceleration data, it is optimistic that IMU acceleration data could be equally as accurate. Future research should continue to study the classification of different tasks and the classification of different skill levels using IMU systems with the goal of developing the knowledge and ability to classify true in-game data. This could provide athletes, coaches, trainers, and spectators with both real-time and seasonal information on player performance of skating tasks.

References

- Boer, R. W., de, & Nilsen, K. L. (1989). The Gliding and Push-off Technique of Male and Female Olympic Speed Skaters. *International Journal of Sport Biomechanics*, 5, 119-134.
- Bracko, M. R., Fellingham, G. W., Hall, L. T., Fisher, A. G., & Cryer, W. (1998). Performance skating characteristics of professional ice hockey forwards. *Sports Medicine, Training and Rehabilitation*, 8(3), 251-263. doi:10.1080/15438629809512531
- Buckeridge, E., LeVangie, M. C., Stetter, B., Nigg, S. R., & Nigg, B. M. (2015). An on-ice measurement approach to analyse the biomechanics of ice hockey skating. *PLoS One*, 10(5), e0127324. doi:10.1371/journal.pone.0127324
- Budarick, A. R., Shell, J. R., Robbins, S. M. K., Wu, T., Renaud, P. J., & Pearsall, D. J. (2018). Ice hockey skating sprints: run to glide mechanics of high calibre male and female athletes. *Sports Biomech*, 1-17. doi:10.1080/14763141.2018.1503323
- Catapault. (2021). Ice Hockey. Retrieved from <https://www.catapultsports.com/sports/ice-hockey>
- Clermont, C. A., Benson, L. C., Osis, S. T., Kobsar, D., & Ferber, R. (2019). Running patterns for male and female competitive and recreational runners based on accelerometer data. *J Sports Sci*, 37(2), 204-211. doi:10.1080/02640414.2018.1488518
- Cust, E. E., Sweeting, A. J., Ball, K., & Robertson, S. (2019). Machine and deep learning for sport-specific movement recognition: a systematic review of model development and performance. *J Sports Sci*, 37(5), 568-600. doi:10.1080/02640414.2018.1521769
- Dixon, P. C., Loh, J. J., Michaud-Paquette, Y., & Pearsall, D. J. (2017). biomechZoo: An open-source toolbox for the processing, analysis, and visualization of biomechanical movement data. *Comput Methods Programs Biomed*, 140, 1-10. doi:10.1016/j.cmpb.2016.11.007
- Dixon, P. C., Schutte, K. H., Vanwanseele, B., Jacobs, J. V., Dennerlein, J. T., Schiffman, J. M., . . . Hu, B. (2019). Machine learning algorithms can classify outdoor terrain types during running using accelerometry data. *Gait Posture*, 74, 176-181. doi:10.1016/j.gaitpost.2019.09.005
- Douglas, A., & Kennedy, C. R. (2019). Tracking In-Match Movement Demands Using Local Positioning System in World-Class Men's Ice Hockey. *The Journal of Strength and Conditioning Research*, 00(00), 1-8.
- Douglas, A., Rotondi, M. A., Baker, J., Jamnik, V. K., & Macpherson, A. K. (2019). On-Ice Physical Demands of World-Class Women's Ice Hockey: From Training to Competition. *Int J Sports Physiol Perform*, 1227-1232. doi:10.1123/ijsp.2018-0571
- Fani, M., & Neher, H. (2017). Hockey Action Recognition via Integrated Stacked Hourglass Network. *IEEE Xplore*.
- Figueiredo, J., Santos, C. P., & Moreno, J. C. (2018). Automatic recognition of gait patterns in human motor disorders using machine learning: A review. *Med Eng Phys*, 53, 1-12. doi:10.1016/j.medengphy.2017.12.006
- Forget, S. (2013). *Comparisons of player calibers and skate models during an ice hockey explosive transitional maneuver*. (Master of Science). McGill University, Montreal QC, Unpublished.
- Fortier, A., Turcotte, R. A., & Pearsall, D. J. (2014). Skating mechanics of change-of-direction manoeuvres in ice hockey players. *Sports Biomech*, 13(4), 341-350. doi:10.1080/14763141.2014.981852
- Garreta, R., & Moncecchi, G. (2013). *Learning scikit-learn: Machine Learning in Python*. Birmingham, UK: Packt Publishing Ltd.
- Genuer, R., Poggi, J.-M., & Tuleau, C. (2008). Random Forests: some methodological insights. *arXiv preprint arXiv:0811.3619*.

- Halilaj, E., Rajagopal, A., Fiterau, M., Hicks, J. L., Hastie, T. J., & Delp, S. L. (2018). Machine learning in human movement biomechanics: Best practices, common pitfalls, and new opportunities. *J Biomech*, 81, 1-11. doi:10.1016/j.jbiomech.2018.09.009
- Hallihan, A. (2018). *Analysis of Male and Female Hockey Players during a Stop and Go Skating Task*. (Master of Science). McGill University, Montreal, QC. eScholar database.
- Hardegger, M., Ledergerber, B., Mutter, S., Vogt, C., Seiter, J., Calatroni, A., & Troster, G. (2015). *Sensor Technology for Ice Hockey and Skating*. Paper presented at the 12th International Conference on Wearable and Implantable Body Sensor Networks (BSN), Cambridge, MA.
- Hastie, T. J., Rosset, S., Tibshirani, R., & Zhu, J. (2004). The Entire Regularization Path for the Support Vector Machine. *Journal of Machine Learning Research*(5), 1391-1415
- Hulin, B. T., Gabbett, T. J., Lawson, D. W., Caputi, P., & Sampson, J. A. (2016). The acute:chronic workload ratio predicts injury: high chronic workload may decrease injury risk in elite rugby league players. *Br J Sports Med*, 50(4), 231-236. doi:10.1136/bjsports-2015-094817
- IIHF. (2021). Survey of Players. Retrieved from <https://www.iihf.com/en/static/5324/survey-of-players>
- Jang, J., Ankit, A., Kim, J., Jang, Y. J., Kim, H. Y., Kim, J. H., & Xiong, S. (2018). A Unified Deep-Learning Model for Classifying the Cross-Country Skiing Techniques Using Wearable Gyroscope Sensors. *Sensors (Basel)*, 18(11). doi:10.3390/s18113819
- Janidarmian, M., Roshan Fekr, A., Radecka, K., & Zilic, Z. (2017). A Comprehensive Analysis on Wearable Acceleration Sensors in Human Activity Recognition. *Sensors (Basel)*, 17(3). doi:10.3390/s17030529
- Kinduct. (2021). Data Consolidation and Integrations. Retrieved from <https://www.kinduct.com/platform/data-consolidation-integrations/>
- Koning, J. J., de, Thomas, R., Berger, M., Groot, G., de, & Ingen Schenau, G. J., van. (1995). The start in speed skating: from running to. *Medicine and Science in Sport and Exercise*, 27(12), 1703-1708.
- Lafontaine, D. (2007). Three-dimensional kinematics of the knee and ankle joints for three consecutive push-offs during ice hockey skating starts. *Sports Biomech*, 6(3), 391-406. doi:10.1080/14763140701491427
- Larson, P. (2003). Global Positioning System and Sport-Specific Testing. *Sports Med*, 33(15), 1093-1101.
- Lu, W.-L., Okuma, K., & Little, J. J. (2009). Tracking and recognizing actions of multiple hockey players using the boosted particle filter. *Image and Vision Computing*, 27(1-2), 189-205. doi:10.1016/j.imavis.2008.02.008
- Luteberget, L. S., Spencer, M., & Gilgien, M. (2018). Validity of the Catapult ClearSky T6 Local Positioning System for Team Sports Specific Drills, in Indoor Conditions. *Front Physiol*, 9, 115. doi:10.3389/fphys.2018.00115
- Mannini, A., & Sabatini, A. M. (2010). Machine learning methods for classifying human physical activity from on-body accelerometers. *Sensors (Basel)*, 10(2), 1154-1175. doi:10.3390/s100201154
- Marino, G. W. (1983). Selected Mechanical Factors Associated with Acceleration in Ice Skating. *Research Quarterly for Exercise and Sport*, 54(3), 234-238. doi:10.1080/02701367.1983.10605301
- McPhee, B. J. (2018). *Study of Soft Exoskeleton with Elastic Assistance on Ice Hockey Forward Skating Acceleration*. (Master of Science). McGill University, Montreal, QC. eScholar database.

- McPherson, M. N., Wrigley, A., & Montelpare, W. J. (2004). The Biomechanical Characteristics of Development-Age Hockey Players: Determining the Effects of Body Size on the Assessment of Skating Techniques. In D. J. Pearsall & A. B. Ashare (Eds.), *Safety in Ice Hockey: Fourth Volume* (pp. 272-287). West Conshohocken, PA: ASTM International.
- Mendes, J. J., Jr., Vieira, M. E., Pires, M. B., & Stevan, S. L., Jr. (2016). Sensor Fusion and Smart Sensor in Sports and Biomedical Applications. *Sensors (Basel)*, 16(10). doi:10.3390/s16101569
- Montgomery, D., Nobes, K., Pearsall, D., & Turcotte, R. (2004). Task Analysis (Hitting, Shooting, Passing and Skating) of Professional Hockey Players. In D. Pearsall & A. B. Ashare (Eds.), *Safety in Ice Hockey* (Vol. 4th, pp. 288-295). West Conshohocken, PA: ASTM International.
- Panebianco, G. P., Bisi, M. C., Stagni, R., & Fantozzi, S. (2018). Analysis of the performance of 17 algorithms from a systematic review: Influence of sensor position, analysed variable and computational approach in gait timing estimation from IMU measurements. *Gait Posture*, 66, 76-82. doi:10.1016/j.gaitpost.2018.08.025
- Pearsall, D. J., Turcotte, R., Lefebvre, R., Bateni, H., Nicolaou, M., Montgomery, D., & Chang, R. (2001). *Kinematics of the foot ankle in forward ice hockey skating*. Paper presented at the Biomechanics Symposia, Univeristy of San Francisco.
- Pearsall, D. J., Turcotte, R. A., & Murphy, S. D. (2000). Biomechanics of Ice Hockey. In *Exercise and Sport Science* (pp. 675-692). Philidelphia: Lippincott Williams & Wilkins.
- Pedregosa, F., Varoquaux, G., Gramfort, A., Michel, V., Thirion, B., Grisel, O., . . . Cournapeau, D. (2011). Scikit-learn: Machine Learning in Python. *Journal of Machine Learning Research*, 12(2011), 2825-2830.
- Pilotti-Riley, A., Stojanov, D., Sohaib Arif, M., & McGregor, S. J. (2019). Video corroboration of player incurred impacts using trunk worn sensors among national ice-hockey team members. *PLoS One*, 14(6), e0218235. doi:10.1371/journal.pone.0218235
- Rakotomamonjy, A. (2003). Variable Selection Using SVM-based Criteria. *Journal of Machine Learning Research*(3), 1357-1370.
- Renaud, P. J., Robbins, S. M. K., Dixon, P. C., Shell, J. R., Turcotte, R. A., & Pearsall, D. J. (2017). Ice hockey skate starts: a comparison of high and low calibre skaters. *Sports Engineering*, 20(4), 255-266. doi:10.1007/s12283-017-0227-0
- Rindal, O. M. H., Seeberg, T. M., Tjonnas, J., Haugnes, P., & Sandbakk, O. (2017). Automatic Classification of Sub-Techniques in Classical Cross-Country Skiing Using a Machine Learning Algorithm on Micro-Sensor Data. *Sensors (Basel)*, 18(1). doi:10.3390/s18010075
- Robbins, S. M., Renaud, P. J., MacInnis, N., & Pearsall, D. J. (2020). The relationship between trunk rotation and shot speed when performing ice hockey wrist shots. *J Sports Sci*, 1-9. doi:10.1080/02640414.2020.1853336
- Sakurai, Y., Fujita, Z., & Ishige, Y. (2016). Automatic Identification of Subtechniques in Skating-Style Roller Skiing Using Inertial Sensors. *Sensors (Basel)*, 16(4). doi:10.3390/s16040473
- Schepers, M., Giuberti, M., & Bellusci, G. (2018). *Xsens MVN: Consistent Tracking of Human Motion Using Inertial Sensing*. Retrieved from Enschede, Netherlands:
- Schulte, O., Khademi, M., Gholami, S., Zhao, Z., Javan, M., & Desaulniers, P. (2017). A Markov Game model for valuing actions, locations, and team performance in ice hockey. *Data Mining and Knowledge Discovery*, 31(6), 1735-1757. doi:10.1007/s10618-017-0496-z
- Scott, M. T. U., Scott, T. J., & Kelly, V. G. (2015). The Validity and Reliability of Global Positioning Systems in Team Sports: A Brief Review. *JSCR*, 30(5), 1470-1490.

- Serpiello, F. R., Hopkins, W. G., Barnes, S., Tavrou, J., Duthie, G. M., Aughey, R. J., & Ball, K. (2018). Validity of an ultra-wideband local positioning system to measure locomotion in indoor sports. *J Sports Sci*, 36(15), 1727-1733. doi:10.1080/02640414.2017.1411867
- Shell, J. R., Robbins, S. M. K., Dixon, P. C., Renaud, P. J., Turcotte, R. A., Wu, T., & Pearsall, D. J. (2017). Skating start propulsion: three-dimensional kinematic analysis of elite male and female ice hockey players. *Sports Biomech*, 16(3), 313-324. doi:10.1080/14763141.2017.1306095
- SPORTLOGiQ. (2021). Hockey. Retrieved from <https://sportlogiq.com/en/>
- Srinivasan, V., Eswaran, C., & Sriraam, N. (2007). Approximate entropy-based epileptic EEG detection using artificial neural networks. *IEEE Trans Inf Technol Biomed*, 11(3), 288-295. doi:10.1109/titb.2006.884369
- Stetter, B. J., Buckeridge, E., Nigg, S. R., Sell, S., & Stein, T. (2019). Towards a wearable monitoring tool for in-field ice hockey skating performance analysis. *Eur J Sport Sci*, 19(7), 893-901. doi:10.1080/17461391.2018.1563634
- Stetter, B. J., Buckeridge, E., von Tscharn, V., Nigg, S. R., & Nigg, B. M. (2016). A Novel Approach to Determine Strides, Ice Contact, and Swing Phases During Ice Hockey Skating Using a Single Accelerometer. *J Appl Biomech*, 32(1), 101-106. doi:10.1123/jab.2014-0245
- Stidwill, T. J., Turcotte, R. A., Dixon, P., & Pearsall, D. J. (2010). Force transducer system for measurement of ice hockey skating force. *Sports Engineering*, 12(2), 63-68. doi:10.1007/s12283-009-0033-4
- Vahdatpour, A., Amini, N., & Sarrafzadeh, M. (2011). *On-body Device Localization for Health and Medical Monitoring Application*. Paper presented at the IEEE, Seattle, WA.
- Vrigkas, M., Nikou, C., & Kakadiaris, I. A. (2015). A Review of Human Activity Recognition Methods. *Frontiers in Robotics and AI*, 2. doi:10.3389/frobt.2015.00028
- Wennberg, R. (2004). Collision frequency in elite hockey on North American versus international size rinks. *Can J Neurol Sci*, 31(3), 373-377. doi:10.1017/s0317167100003474
- Wong, T.-T., & Yeh, P.-Y. (2020). Reliable Accuracy Estimates from k-Fold Cross Validation. *IEEE Transactions on Knowledge and Data Engineering*, 32(8), 1586-1594. doi:10.1109/tkde.2019.2912815
- Zhang, C., & Ma, Y. (Eds.). (2012). *Ensemble Machine Learning - Methods and Applications*. New York, NY, USA: Springer.
- Zhao, J. (2018). A Review of Wearable IMU (Inertial-Measurment-Unit)-based Pose Estimation and Drift Reduction Technologies. *J. Phys.: Conf. Ser*, 1087.

APPENDICES

Appendix A – Stop & Go Task Visual

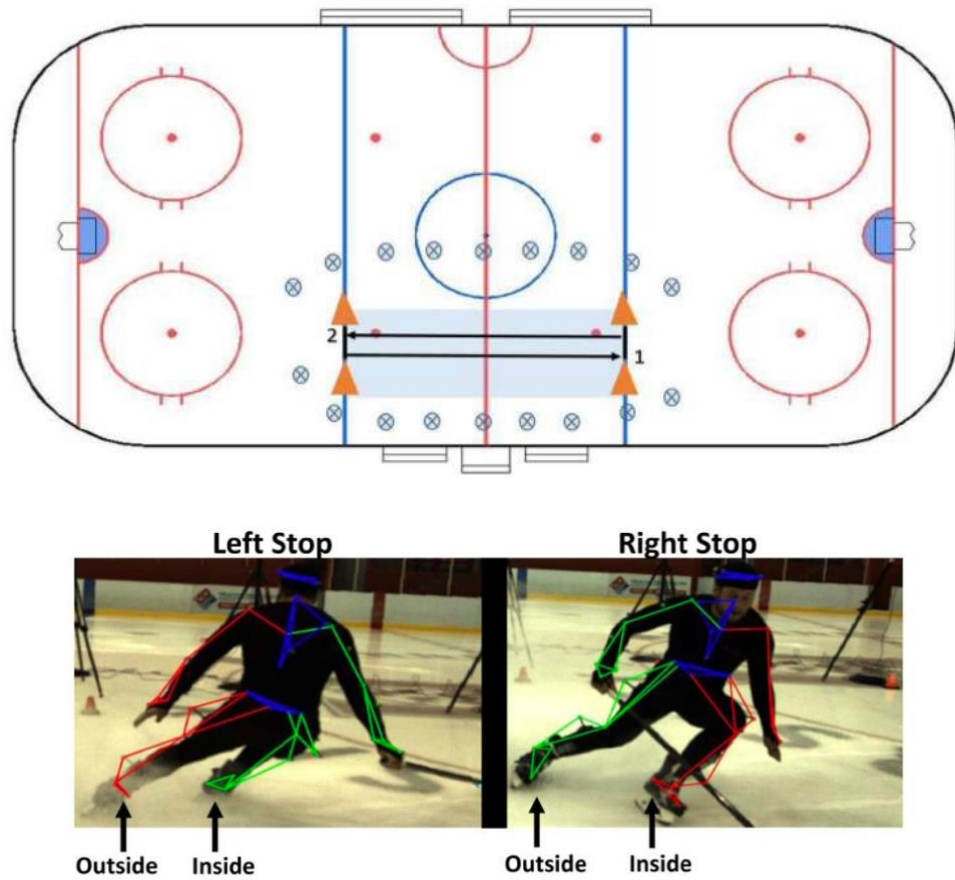


Figure 7 Visual representation of stop & go task from Hallihan (2018).

Appendix B – Skating Start Task Visual

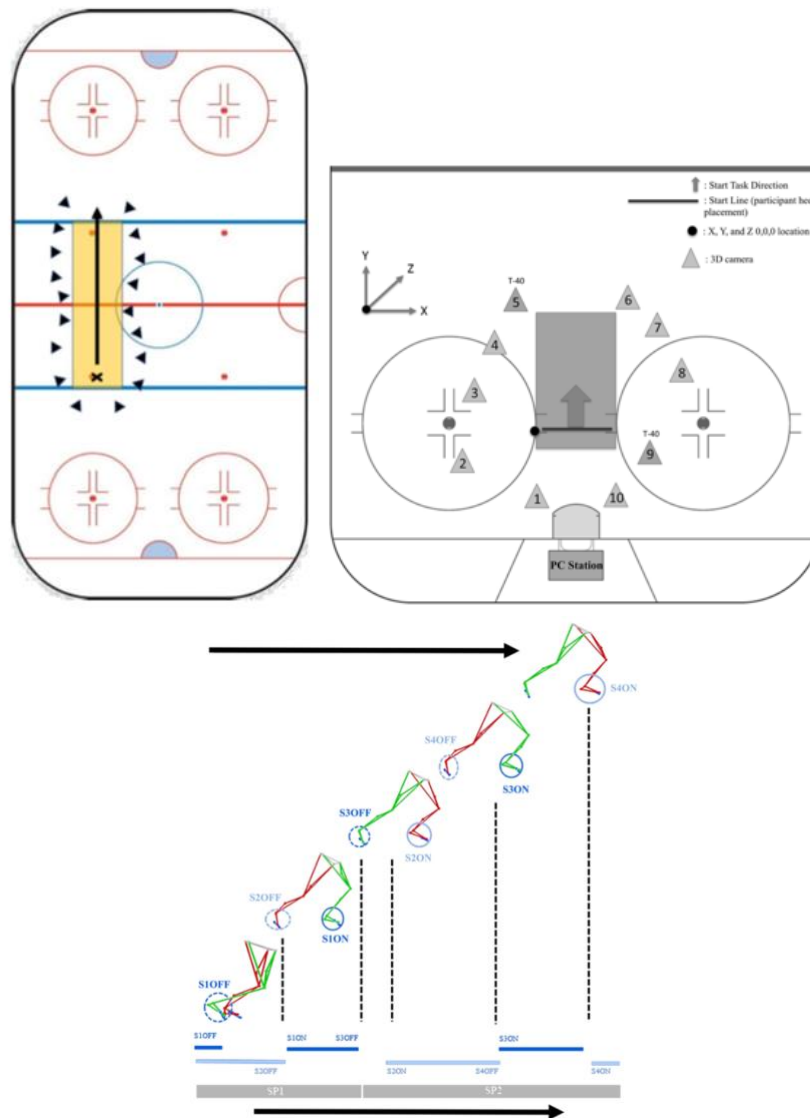


Figure 8 Visual representation of skating start task from Shell et al. (2017) and Renaud et al. (2017)

Appendix C – Skating Stride Task Visual

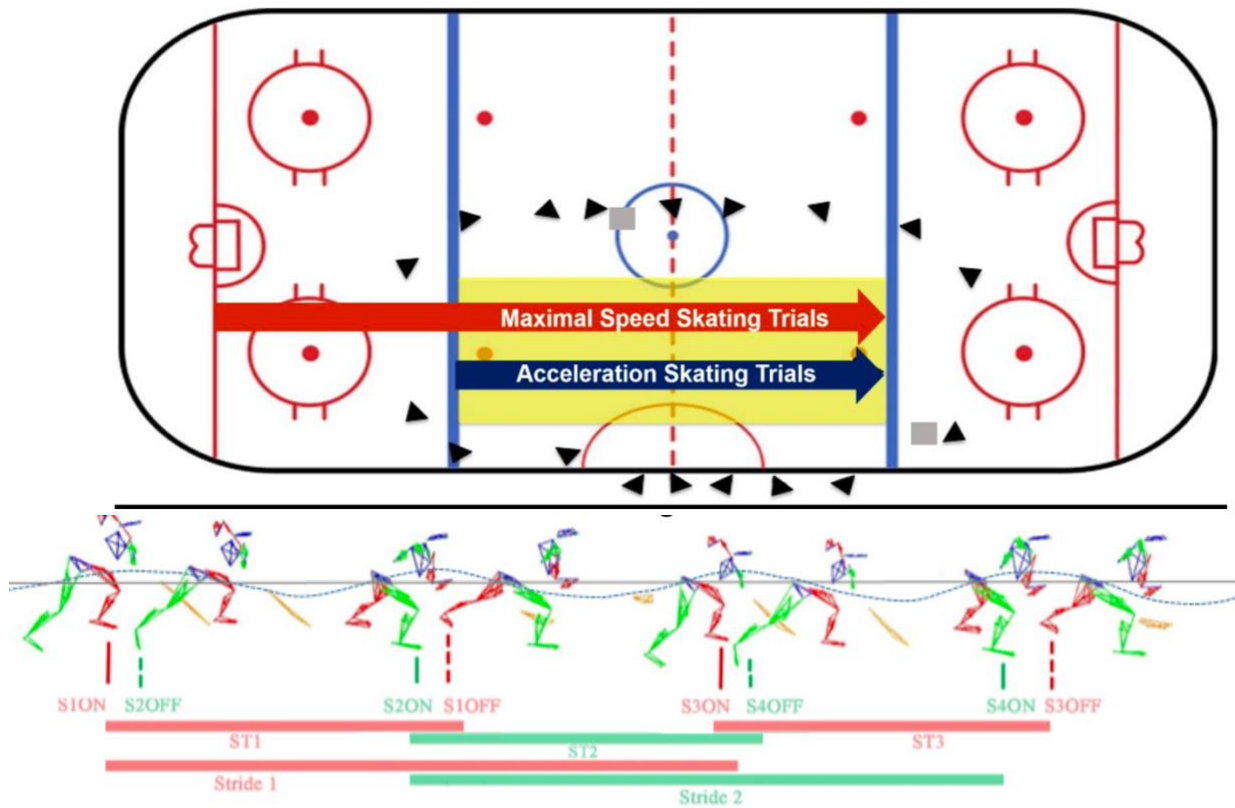


Figure 9 Visual representation of skating stride task from Budarick et al. (2018)

Appendix D – Wrist Shot Task Visual

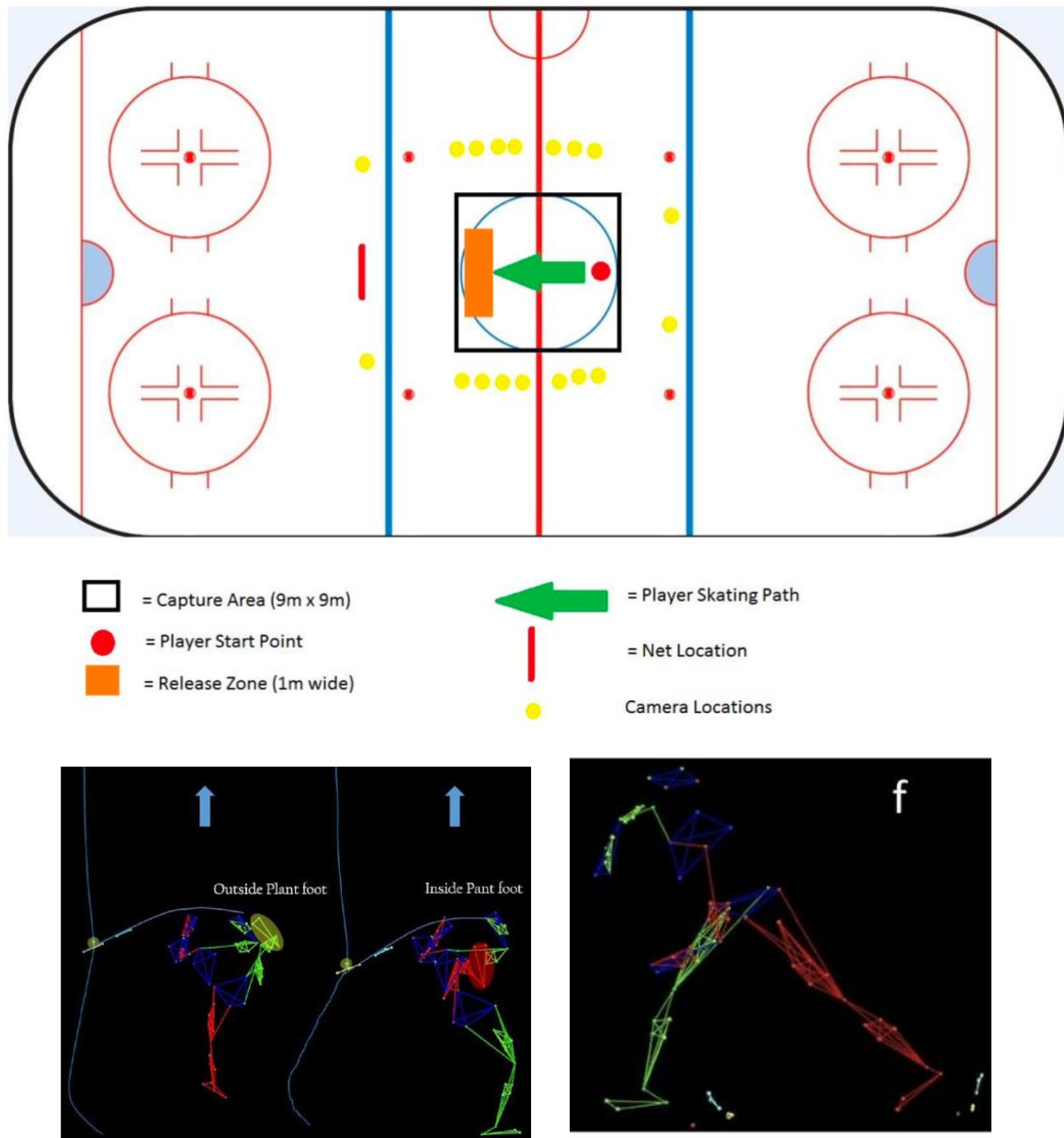
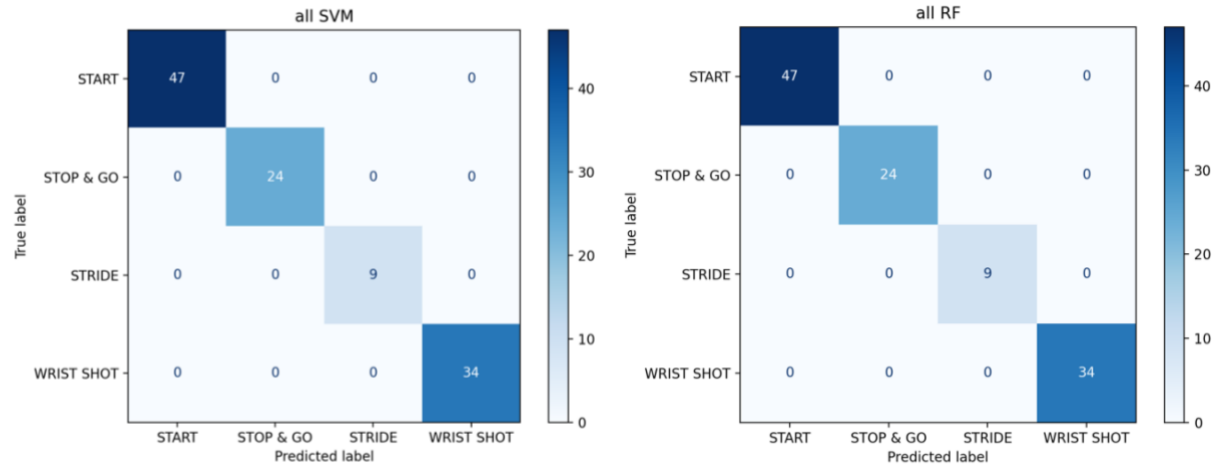


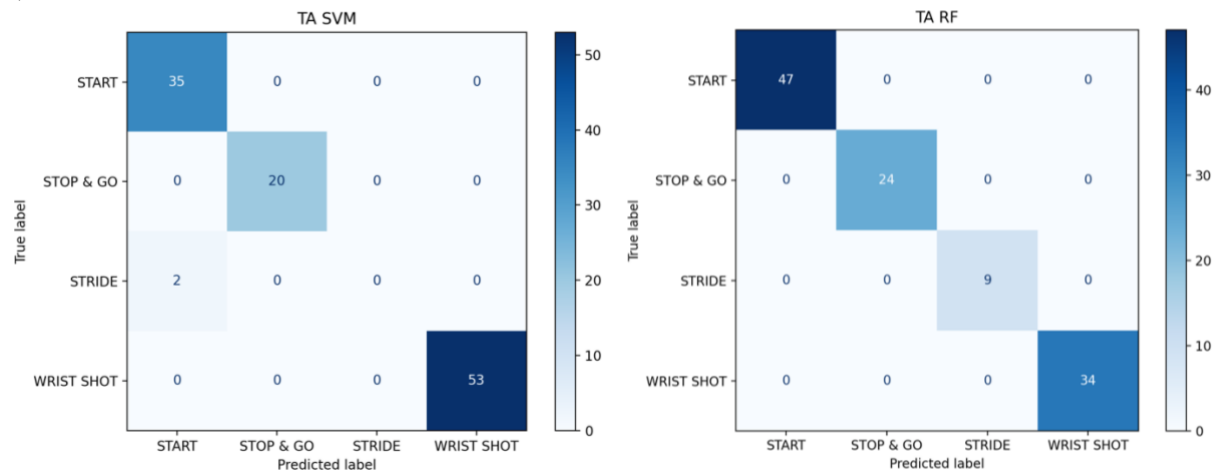
Figure 10 Overhead and sagittal visual representation of wrist shot task from Robbins et al. (2020)

Appendix E – Top Performing Models

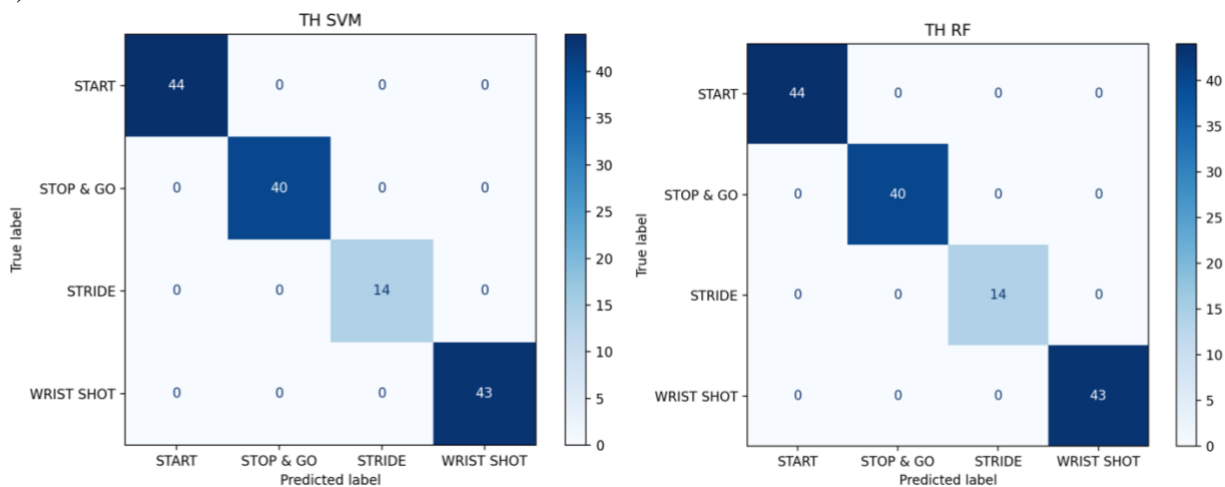
a)



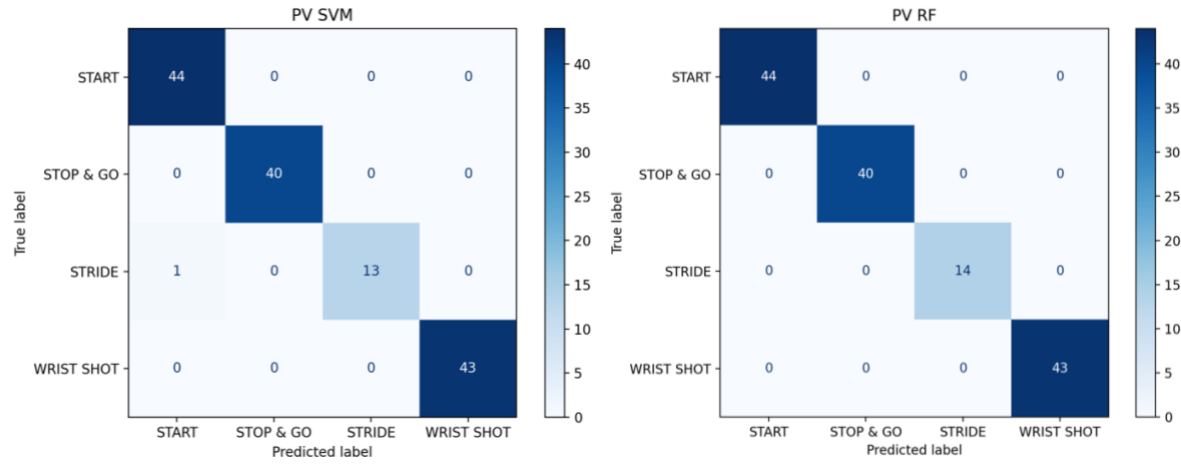
b)



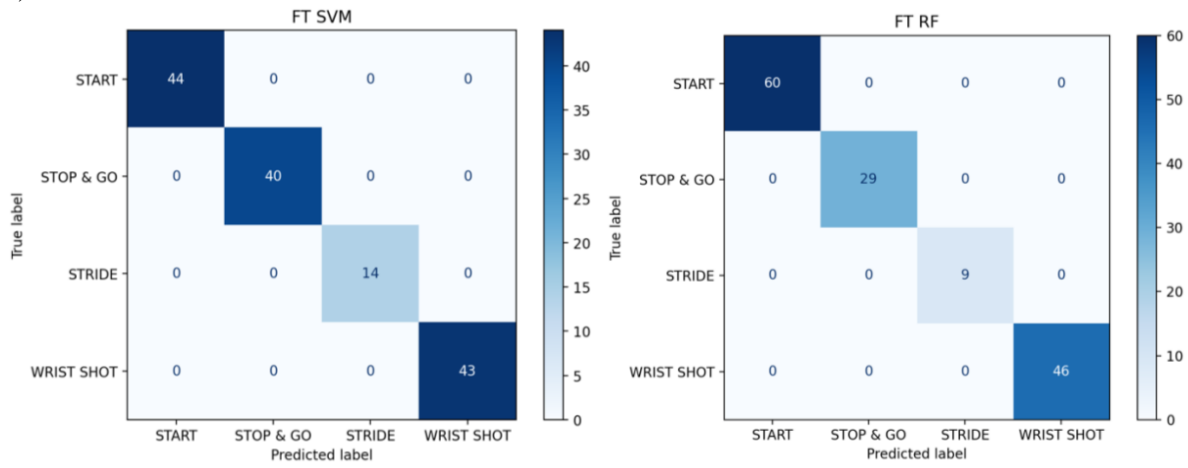
c)



d)



e)



f)

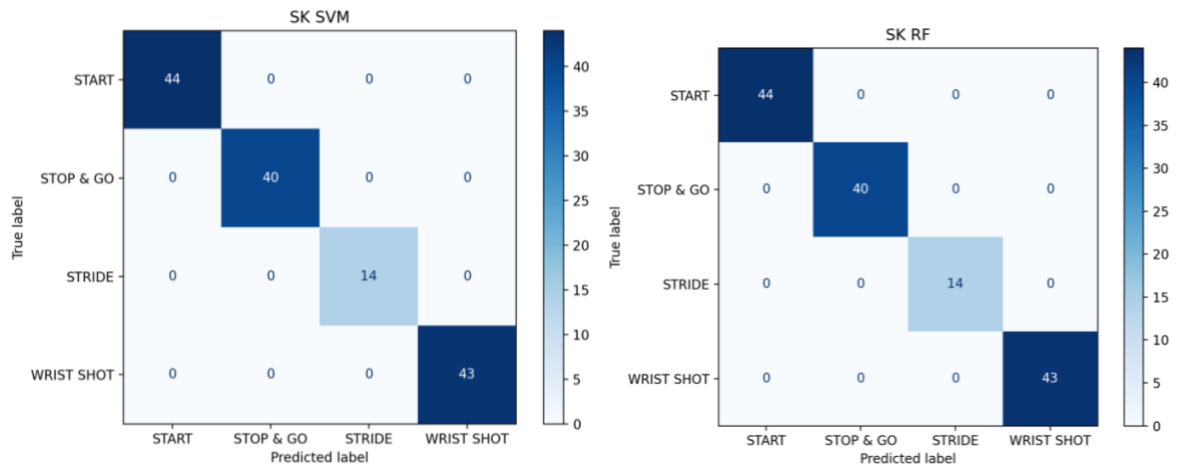
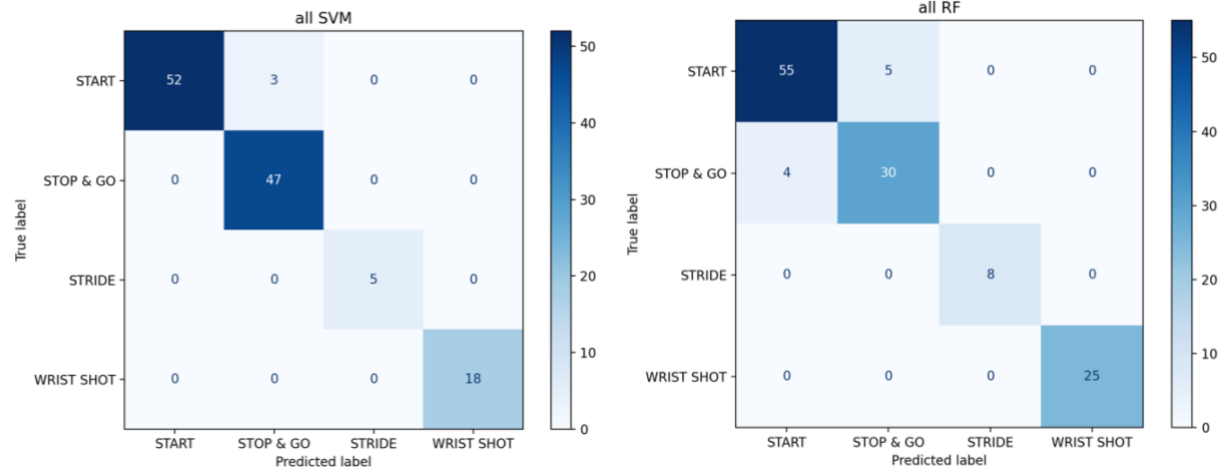


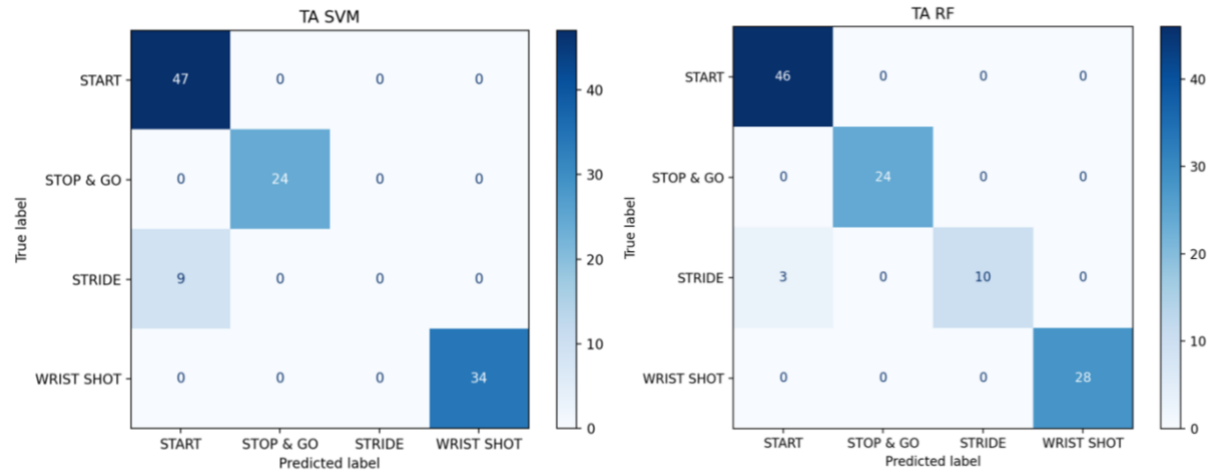
Figure 11 Example confusion matrices of top performing models from the 10-fold cross validation of a) all segments b) trunk segment c) thigh segment d) pelvis segment e) foot segment f) shank segment.

Appendix F – Moderate Performing Models

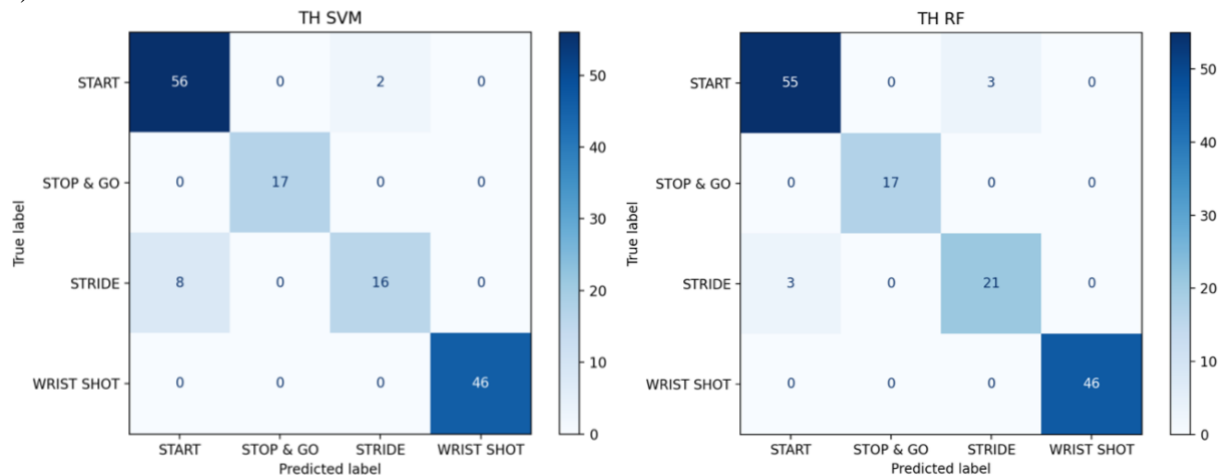
a)



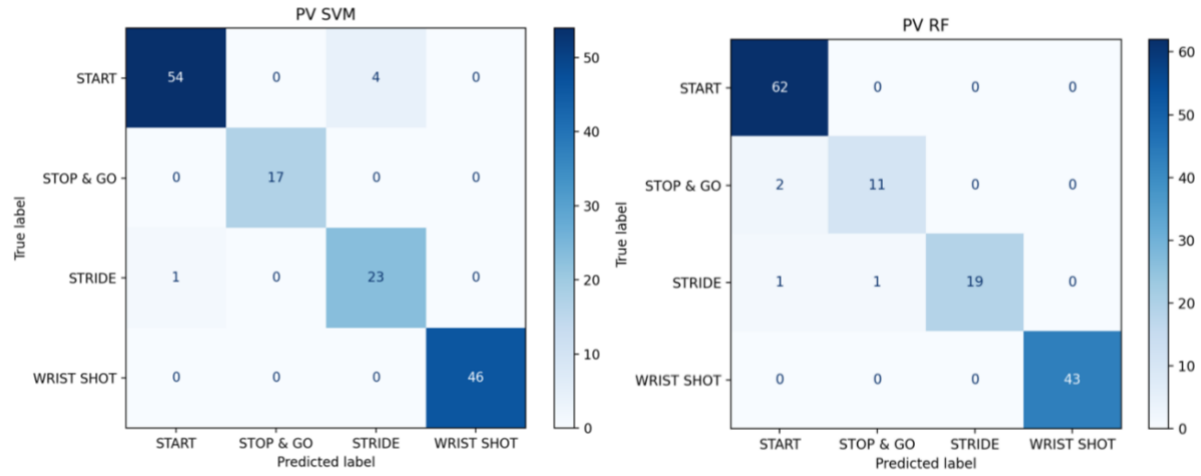
b)



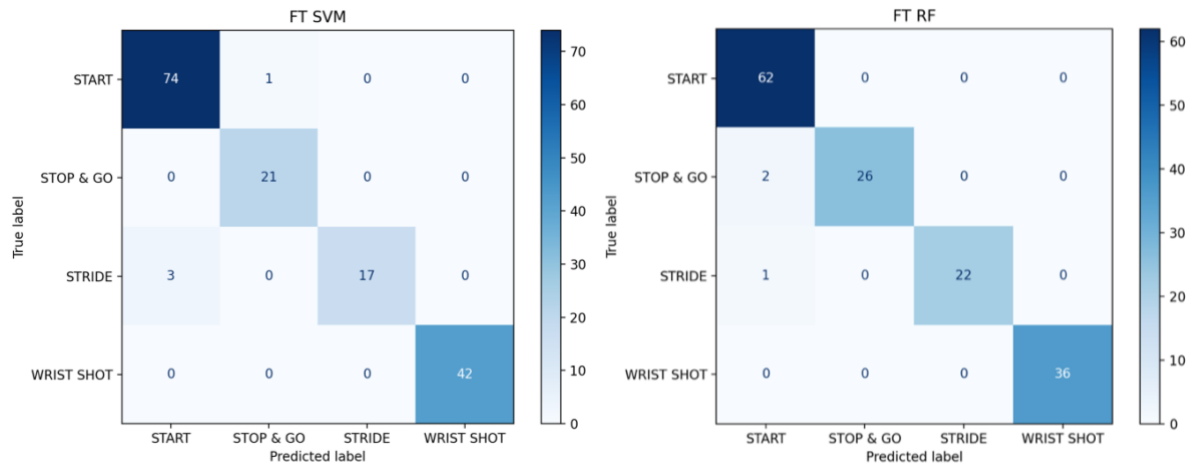
c)



d)



e)



f)

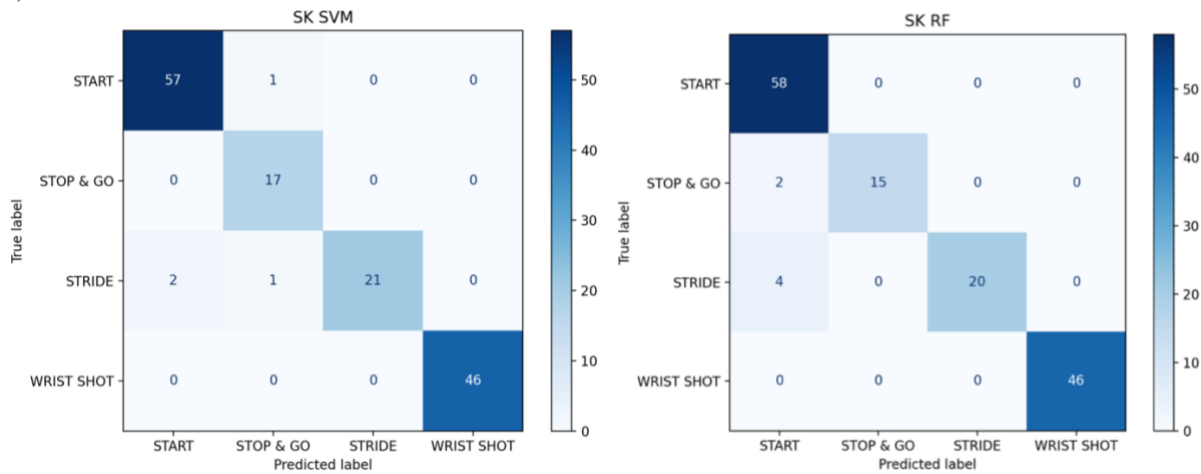
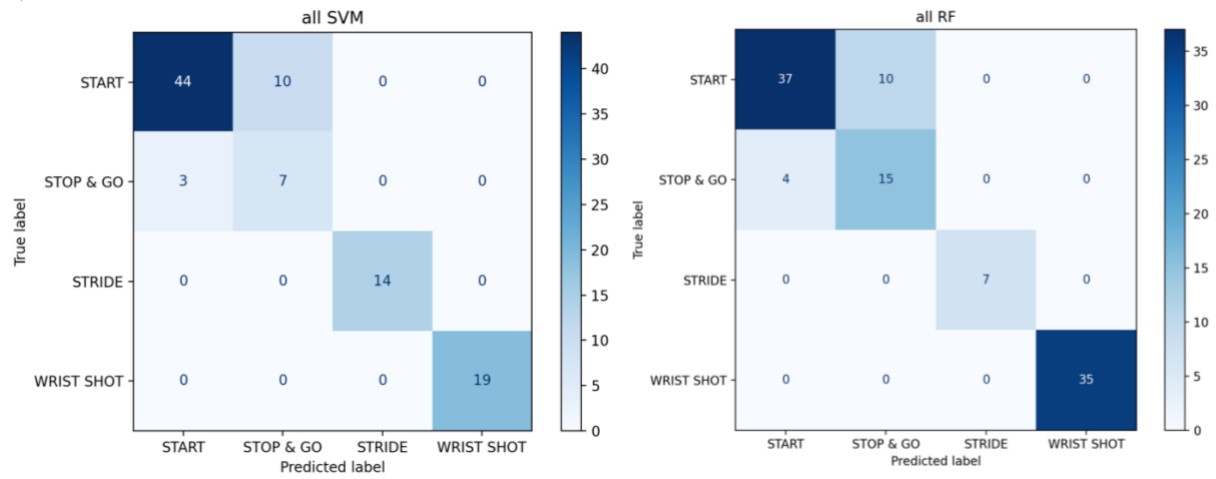


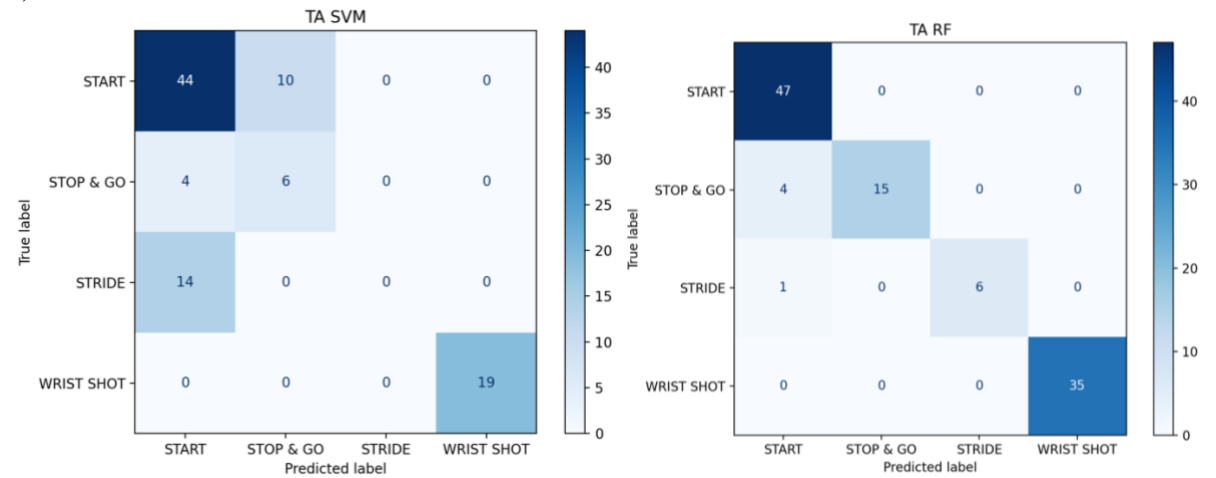
Figure 12 Example confusion matrices of moderate performing models from the 10-fold cross validation of a) all segments b) trunk segment c) thigh segment d) pelvis segment e) foot segment f) shank segment.

Appendix G – Poor Performing Models

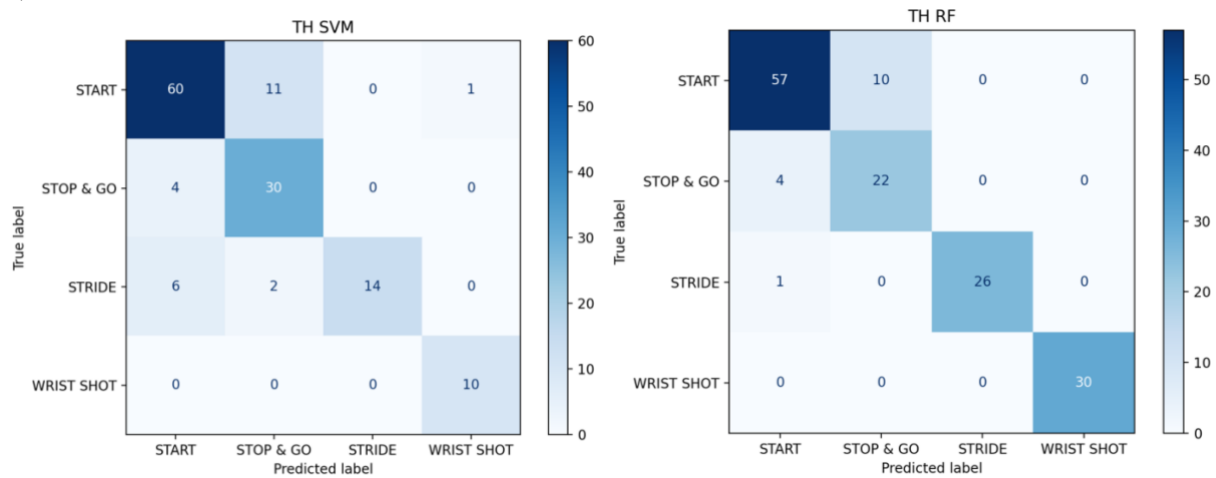
a)



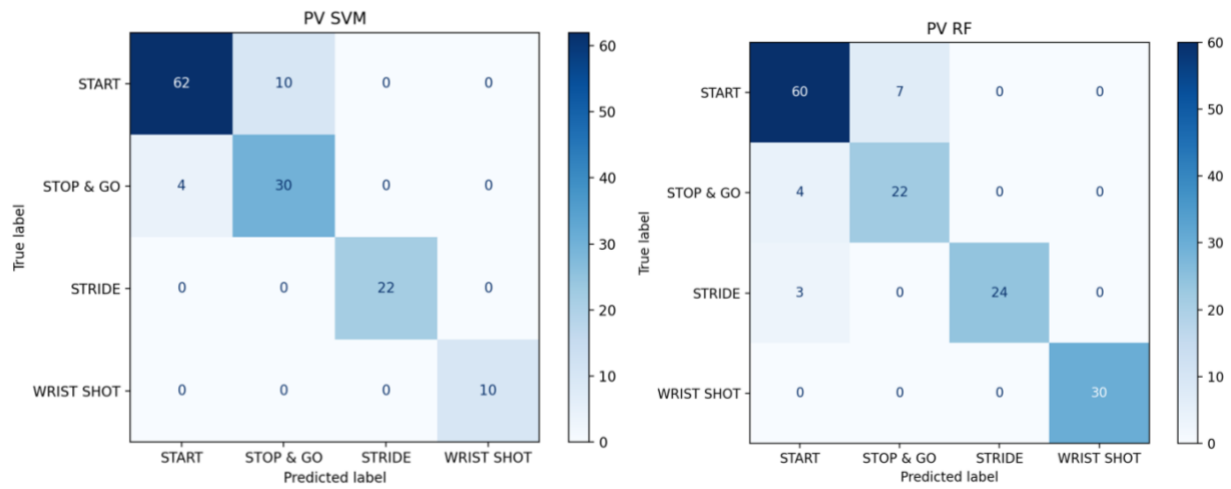
b)



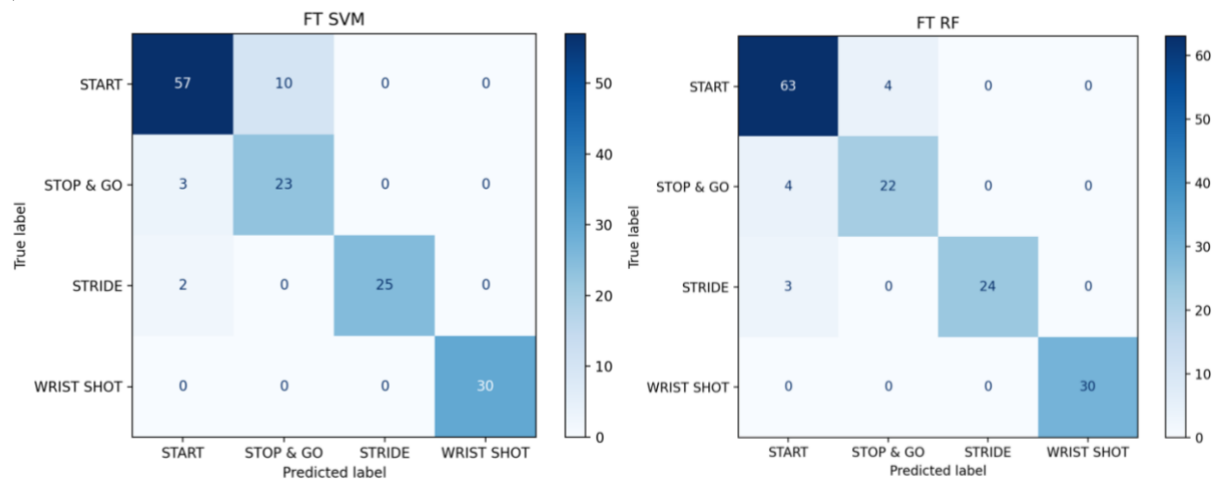
c)



d)



e)



f)

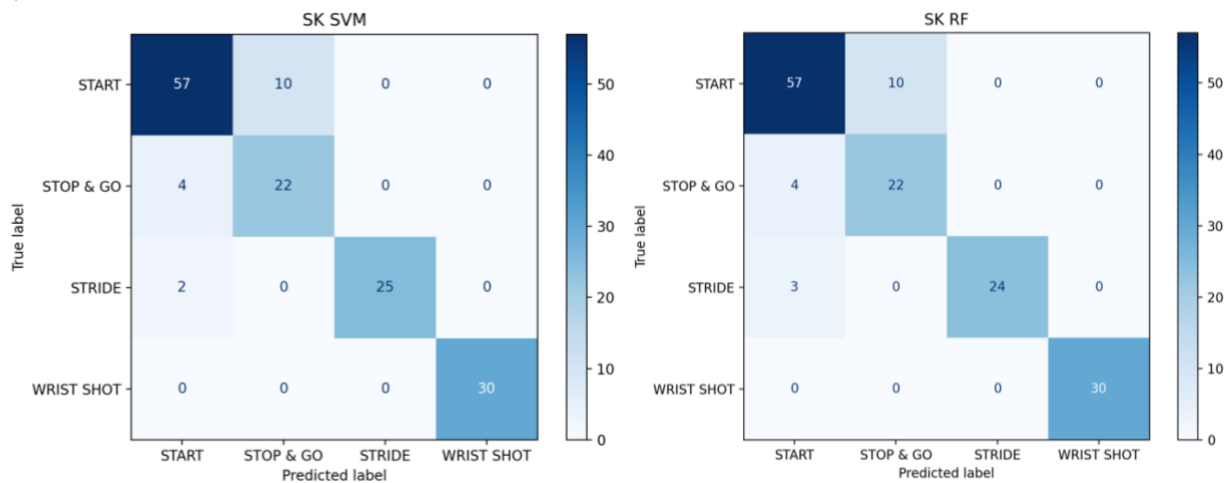
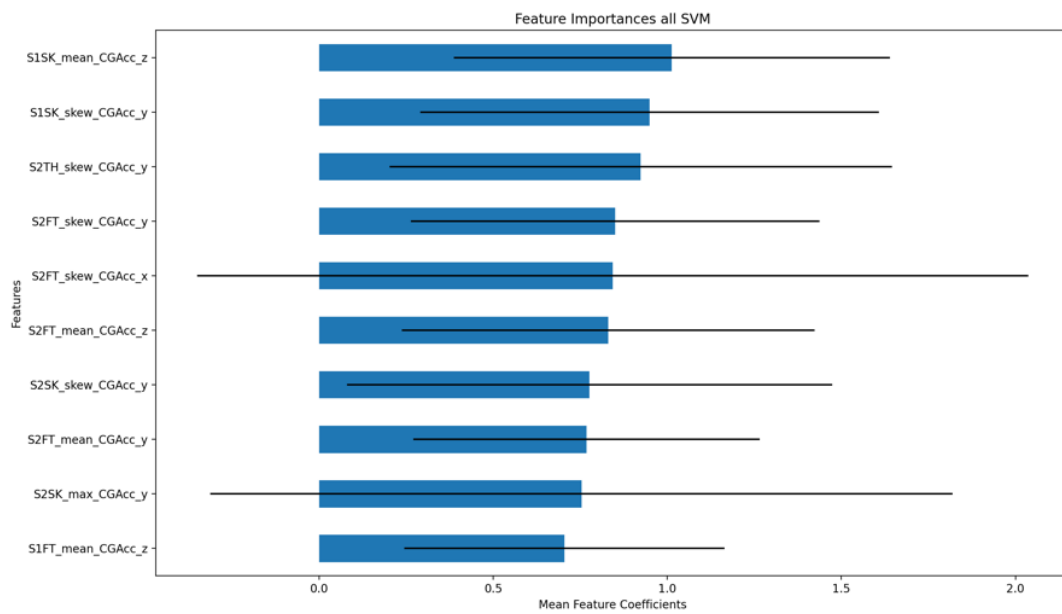


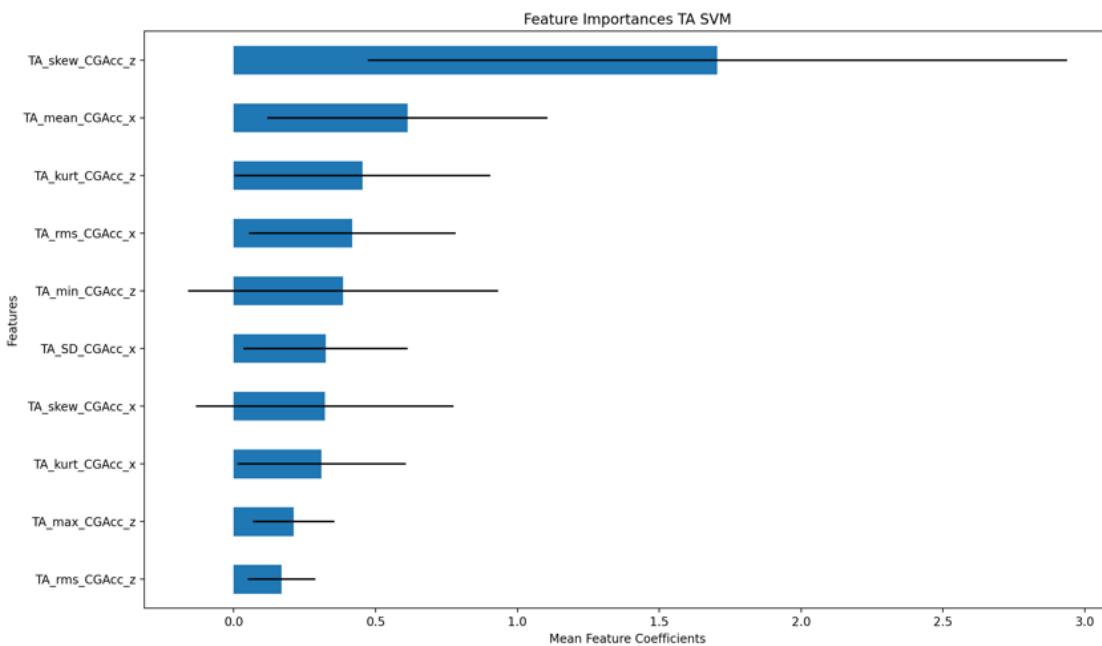
Figure 13 Example confusion matrices of poor performing models from the 10-fold cross validation of a) all segment b) trunk segment c) thigh segment d) pelvis segment e) foot segment f) shank segment.

Appendix H – Feature Importances SVM Model Segments

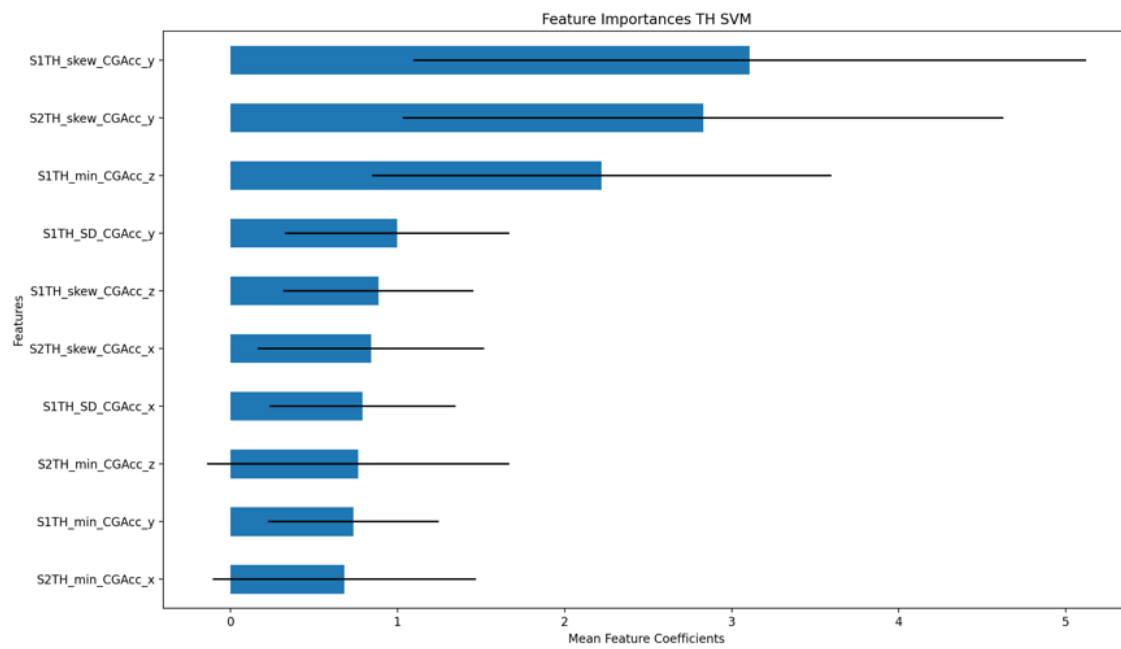
a)



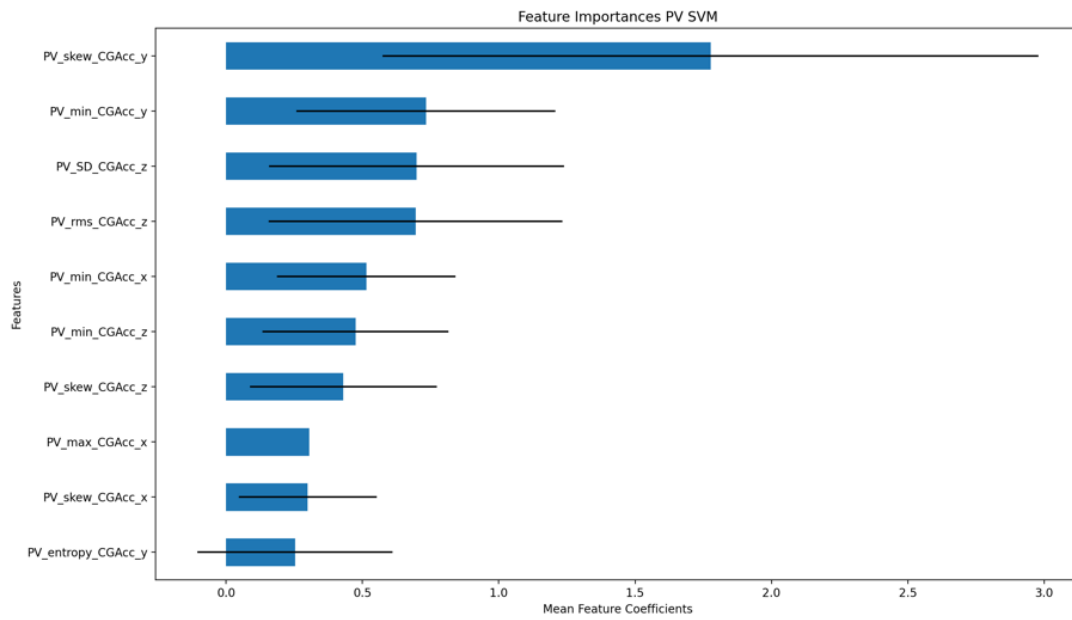
b)



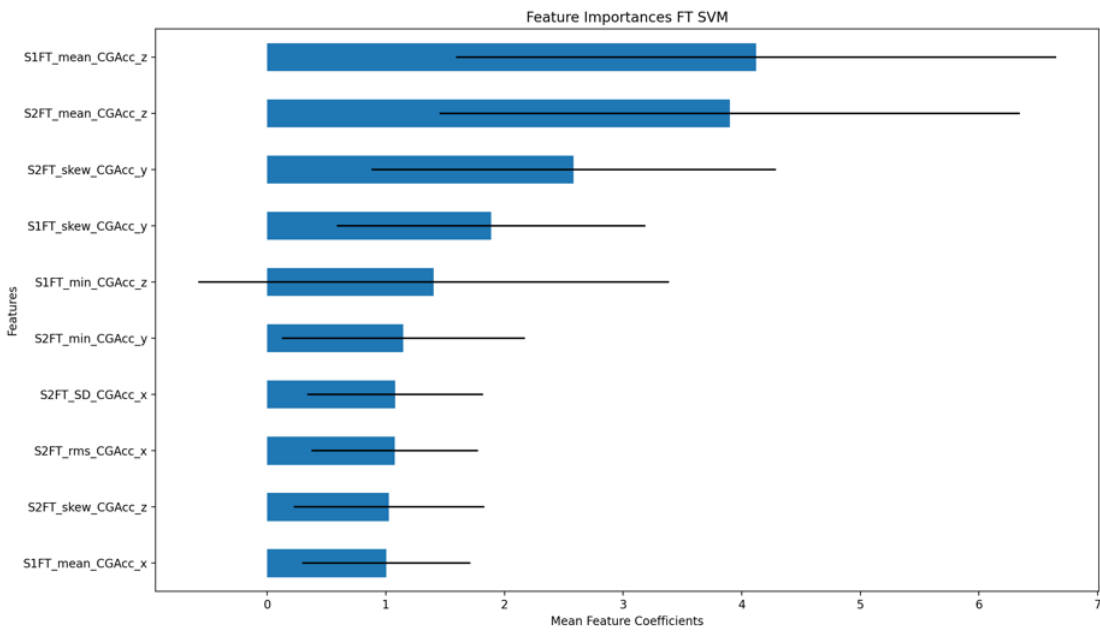
c)



d)



e)



f)

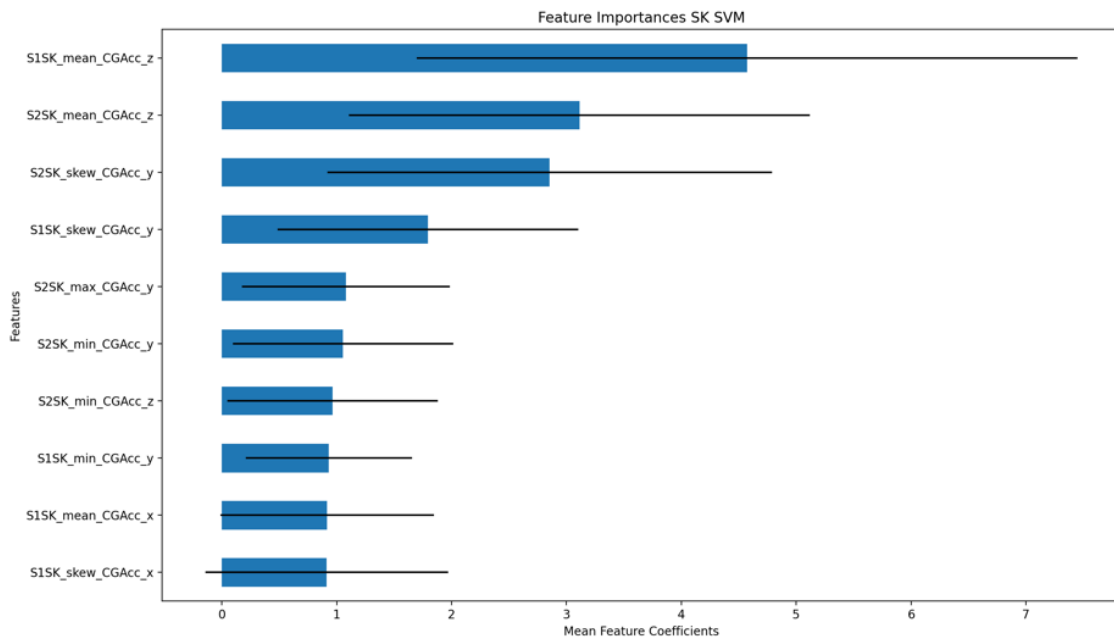
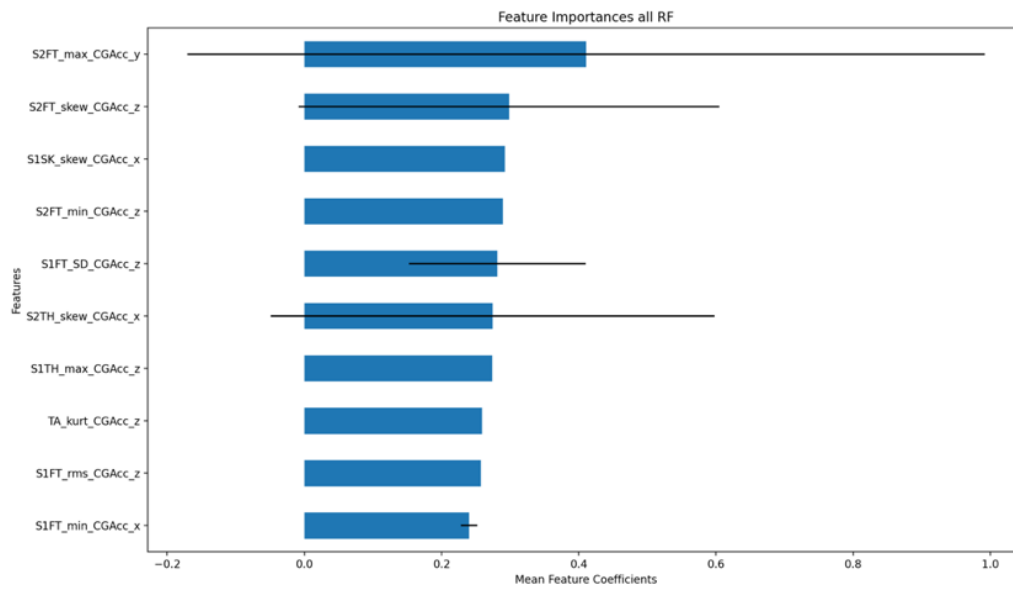


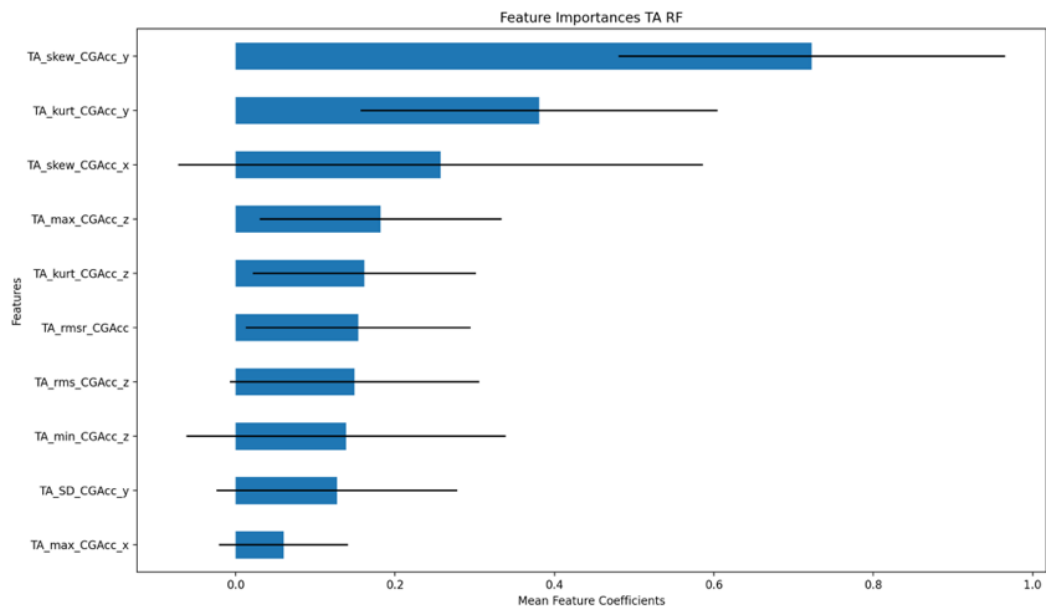
Figure 14 Top 10 feature importances (mean and standard deviation) of the SVM model for a) all segment b) trunk segment c) thigh segment d) pelvis segment e) foot segment f) shank segment.

Appendix I – Feature Importances RF Model Segments

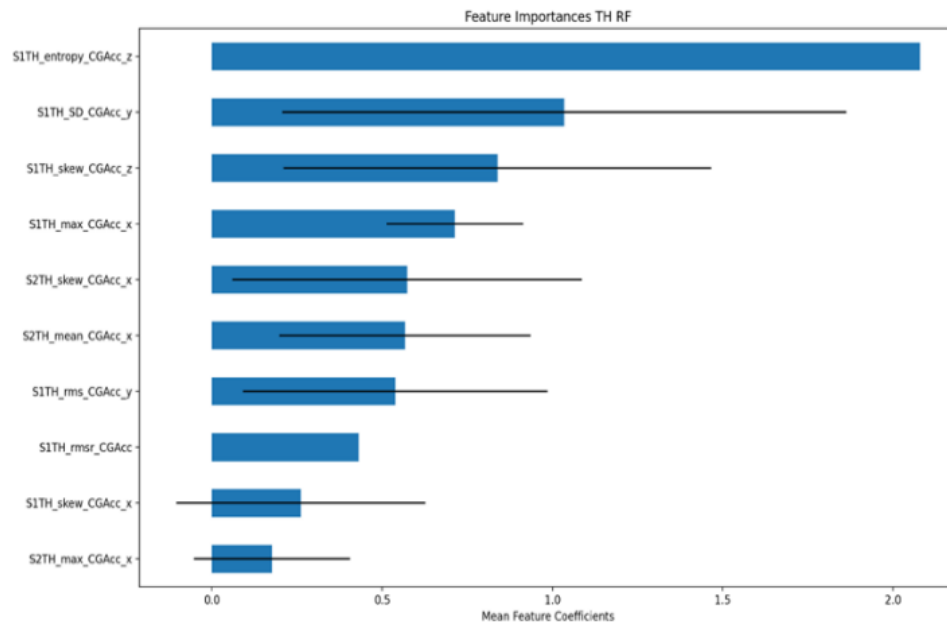
a)



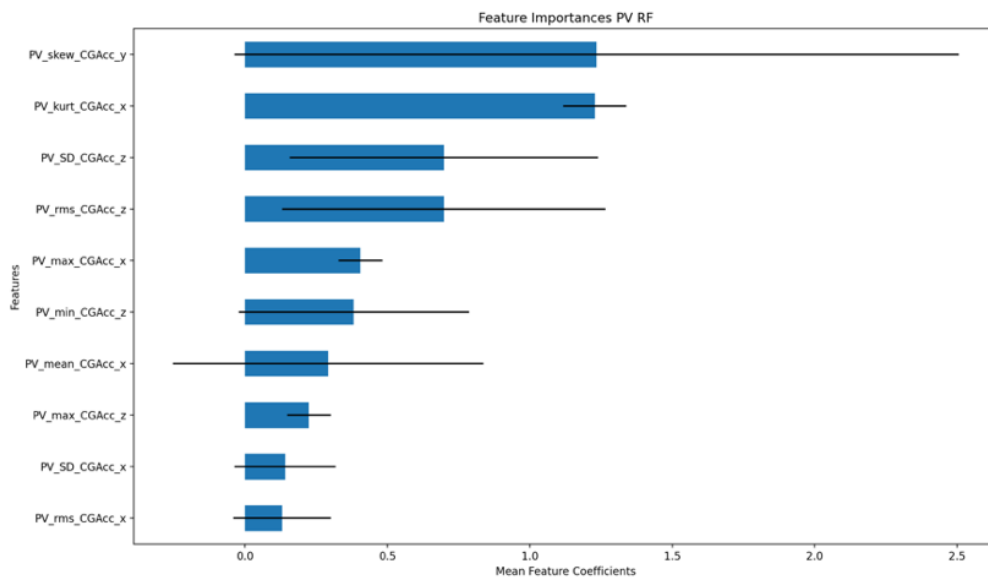
b)



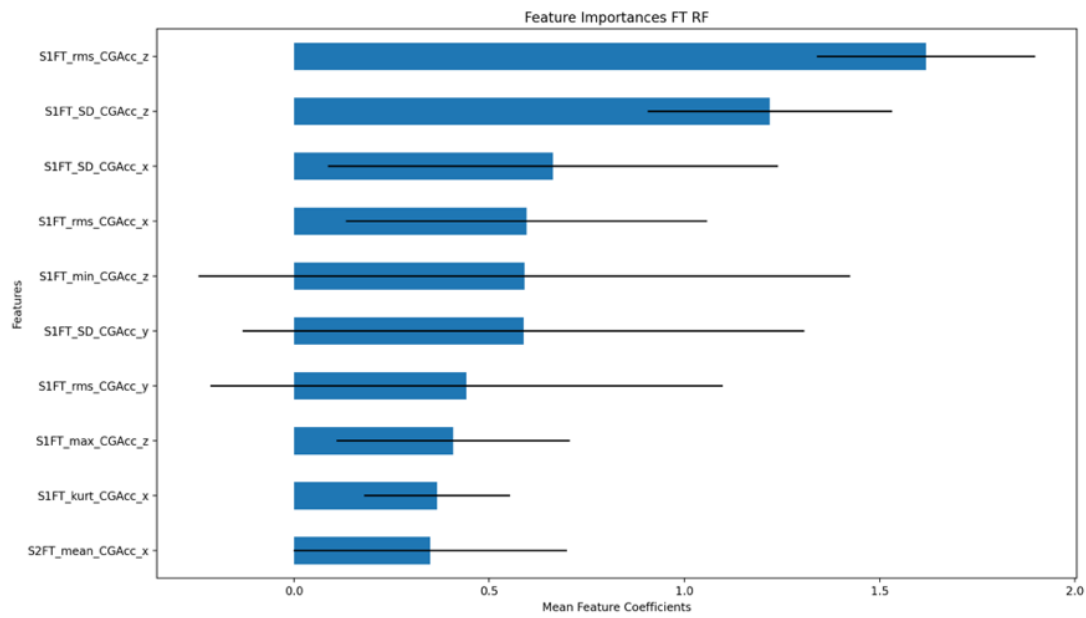
c)



d)



e)



f)

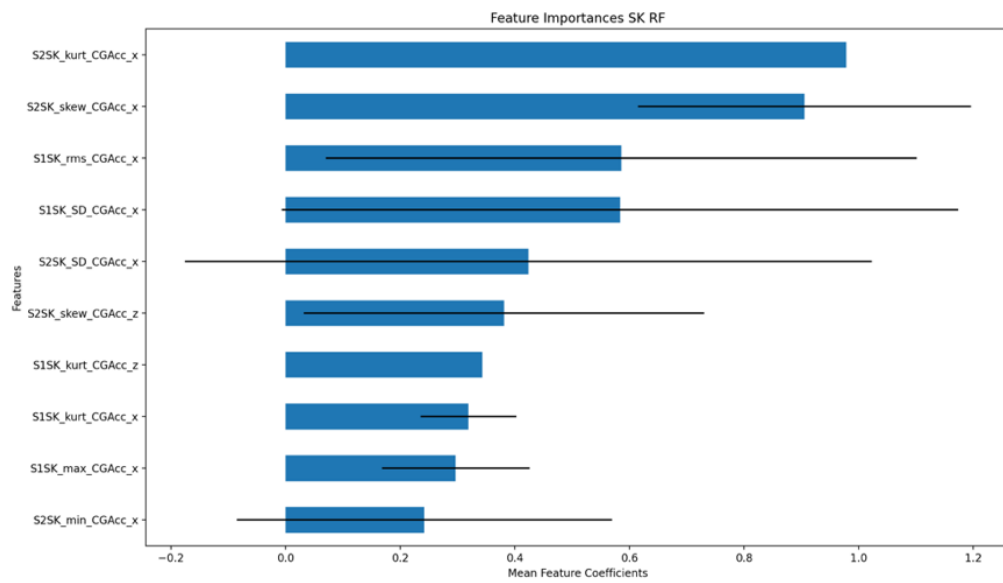


Figure 15 Top 10 feature importances (mean and standard deviation) of the RF model for a) all segment b) trunk segment c) thigh segment d) pelvis segment e) foot segment f) shank segment